Arylethynyl Substituted 9,10-Anthraquinones: Tunable Stokes Shifts by Substitution and Solvent Polarity

Jinhua Yang,[†] Amala Dass,[†] Abdel-Monem M. Rawashdeh,[†] Chariklia Sotiriou-Leventis,*[,†] Matthew J. Panzner,[‡] Daniel S. Tyson,[§] James D. Kinder,[||] and Nicholas Leventis*[,||]

Department of Chemistry, University of Missouri−Rolla, Rolla, Missouri 65409, Department of Chemistry, The University of Akron, Akron, Ohio 44325, Ohio Aerospace Institute, 22800 Cedar Point Road, Cleveland, Ohio 44142, and NASA Glenn Research Center, Materials Division M.S. 49-1, 21000 Brookpark Road, Cleveland, Ohio 44135

Received March 12, 2004. Revised Manuscript Received June 21, 2004

2-Arylethynyl- and 2,6- and 2,7-diarylethynyl-substituted 9,10-anthraquinones were synthesized via Sonogashira coupling reactions of 2-bromo-, 2,6-dibromo-, and 2,7-dibromo-9,10-anthraquinone with para-substituted phenylacetylenes. While the redox properties of those compounds are almost insensitive to substitution, their absorption maxima are linearly related to the Hammett constants with different slopes for electron donors and electron acceptors. All compounds are photoluminescent both in solution (quantum yields of emission ≤6%), and as solids. The emission spectra have the characteristics of charge-transfer bands with large Stokes shifts (100−250 nm). The charge-transfer character of the emitting state is supported by large dipole moment differences between the ground and the excited state as concluded on the basis of molecular modeling and Lippert−Mataga correlations of the Stokes shifts with solvent polarity. Maximum Stokes shifts are attained by both electron-donating and -withdrawing groups. This is explained by a destabilization of the HOMO by electron donors and a stabilization of the LUMO by electron acceptors. X-ray crystallographic analysis of, for example, 2,7-bisphenylethynyl-9,10-anthraquinone reveals a monoclinic $P2_1/n$ space group and no indication for π-overlap that would promote quenching, thus explaining emission from the solid state. Representative reduced forms of the title compounds were isolated as stable acetates of the corresponding dihydro-9,10-anthraquinones. The emission of these compounds is blue-shifted relative to the parent oxidized forms and is attributed to internal transitions in the dihydro-9,10-anthraquinone core.

Introduction

Quinones and their derivatives comprise an important class of redox mediators and electron-transfer quenchers. They are found in the electron transport chain of biological systems and they are involved in photosynthesis of plants and bacteria.[1] In general, quinones are naturally colored and therefore have been used extensively as colorants in the dyestuff industry but also as sensitizers in "phototendering" of cellulose or in the photooxidative degradation of polymeric materials.[2] Currently, quinones are considered together with other traditional colorants for application in technologies such as optical data transmission and storage, bioanalytical probes, and solar energy conversion, which all require absorption and/or emission of long wavelength light, preferably in the near-infrared.[3] Thus, as expected, extending the conjugation of parent naphtha- and anthraquinones by electron donors and/or acceptors pushes the electronic absorption spectrum beyond 700 nm.[3a] On the other hand, photoluminescence from unsubstituted 9,10-anthraquinone itself is generally not observed. Phosphorescence and delayed fluorescence from this compound have been observed only in Freon (1,1,2-trichlorotrifluoroethane), which, due to its chemical inertness, minimizes photochemical reactivity.[4] Unlike 9,10-anthraquinone itself, however, even simple derivatives such as hydroxyl- and amino-substituted 9,10-anthraquinones are known to be photoluminescent. Therefore, it was considered reasonable that arylethynyl-substituted anthraquinones would not only turn out to be photoluminescent but also by extending the conjugation we could first move the photophysical properties to longer wavelengths and we would second realize an additional degree of freedom in tuning those properties through the para-substituents of the aryl group.[5] Thus, we synthesized 2,7-diX, 2,6-diX, and 2-X,

* Corresponding authors. C.S.-L.: e-mail, cslevent@umr.edu; tel, 573-341-4353. N.L.: e-mail, Nicholas.Leventis@nasa.gov; tel, 216-433-3202.
[†] University of Missouri−Rolla.
[‡] The University of Akron.
[§] Ohio Aerospace Institute.
[||] NASA Glenn Research Center.

(1) Poulsen, J. R.; Birks, J. W. *Anal. Chem.* **1989**, *61*, 2267−2276. (b) Görner, H. *Photochem. Photobiol.* **2003**, *77*, 171−179.
(2) Diaz, A. N. *J. Photochem. Photobiol, A: Chem.* **1990**, *53*, 141−167.
(3) Fabian, J.; Nakazumi, H.; Matsuoka, M. *Chem. Rev.* **1992**, *92*, 1197−1226. (b) Kohl, C.; Becker, S.; Müllen, K. *Chem. Commun.* **2002**, 2778−2779. (c) Miller, L. L.; Liberko, C. A. *Chem. Mater.* **1990**, *2*, 339−340.
(4) Carlson, S. A.; Hercules, D. M. *J. Am. Chem. Soc.* **1971**, *93*, 5611−5616.

10.1021/cm049590g CCC: $27.50
Published on Web 08/12/2004

and with the exception of 2,7-diN$(CH_3)_2$, they are all photoluminescent in fluid solution.[2,6] Surprisingly, in the beginning for such rigid systems, all compounds of

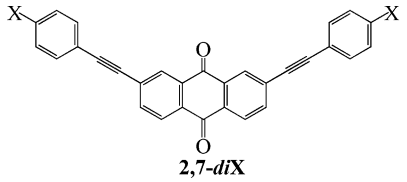

2,7-*di*X

-X = -H, -CH_3, -OCH_3, -SCH_3, -$N(CH_3)_2$, -NO_2, -$COCH_3$, -CH_2CN, -$S(CH_3)_2^+$

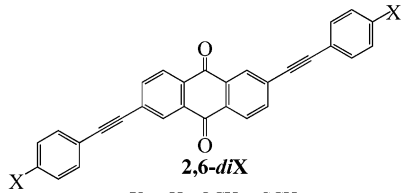

2,6-*di*X

-X = -H, -OCH_3, -SCH_3

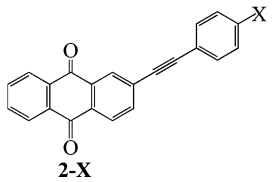

2-X

-X = -H, -CH_3, -OCH_3, -NO_2

this study show large Stokes shifts, (100−250 nm), with *both* strong electron-donating and -withdrawing substituents. It was discovered that the overall large values of the Stokes shifts are due to the charge-transfer character of the emitting excited state, while the relatively smaller variation of the Stokes shifts with substitution has been attributed to the destabilization of the HOMO by electron-donating substituents and the stabilization of the LUMO by electron-withdrawing ones. The charge transfer character of the emitting excited state originates from the fact that the HOMO and the LUMO are located at different regions of the molecules. These results comprise a paradigm, whereas longer emission wavelengths are achieved not only by extending the conjugation but also by introducing charge-transfer transitions by design. In this context, the *p*-substituted phenylethynyl group emerges as an effective molecular tool for such effects. At last, we have also investigated the photoluminescent properties of selected reduced forms, namely those of 2,7-diOCH_3, 2,6-diH, and 2,6-diOCH_3, and we report anthracene-like emission. These findings are discussed in terms of their relevance to novel optoelectronic systems for switching, sensors, and displays based on redox modulation of the emission spectrum.

Results

1. Synthesis of 2,7-diX, 2,6-diX, 2-X, and Selective Reduced Forms. Compounds 2,7-diX, 2,6-diX, and 2-X

Scheme 1. Synthesis of 2,7-diXs[a]

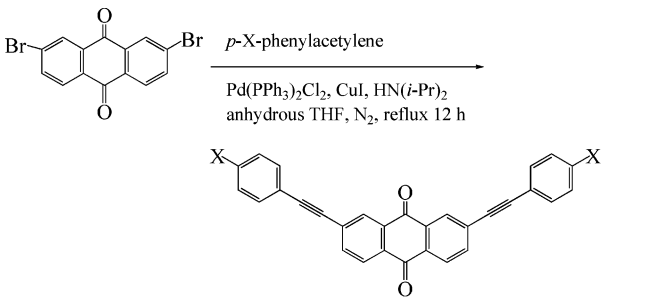

2,7-*di*X

X(% yield) = H(82); CH_3(54); OCH_3(64); SCH_3(40); $N(CH_3)_2$(25); NO_2(56); $COCH_3$(35); CH_2CN(67)

[a] 2,6-diX and 2-Xs were synthesized by identical procedures.

Scheme 2. Synthesis of *p*-N$(CH_3)_2$-phenylacetylene

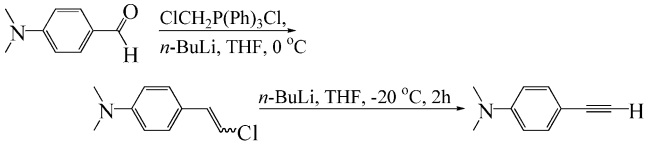

80 % (*cis:trans*=2:1) 96 %

were synthesized via Sonogashira coupling reactions of 2,7-dibromo-, 2,6-dibromo-, and 2-bromo-9,10-anthraquinone, respectively, with the appropriate *p*-substituted phenylacetylenes (Scheme 1). 2,7-di$S(CH_3)_2^+$ was prepared by treating 2,7-diSCH_3 with $(CH_3)_3O^+BF_4^-$.

Of the *p*-substituted phenylacetylenes used in Scheme 1, only the *p*-H and the *p*-OCH_3 homologues are commercially available. The *p*-SCH_3, *p*-CH_3 analogues were available from previous studies.[7] The *p*-$COCH_3$, *p*-NO_2, and *p*-CH_2CN compounds were prepared via Sonogashira coupling reactions of the corresponding commercially available *p*-X-bromobenzenes and (trimethylsilyl)acetylene (in analogy to Scheme 1), followed by deprotection (see Experimental Section). *p*-N$(CH_3)_2$-phenylacetylene was prepared through a Wittig reaction of *p*-dimethylaminobenzaldehyde and (chloromethylene)triphenylphosphorane, followed by treatment with a base (Scheme 2).[8]

2-Bromo-, 2,6-dibromo-, and 2,7-dibromo-9,10-anthraquinones used in Scheme 1 were synthesized from the corresponding amino-substituted 9,10-anthraquinones via Sandmeyer reactions. In turn, 2-amino- and 2,6-diamino-9,10-anthraquinone are commercially available, while 2,7-diamino-9,10-anthraquinone was prepared from anthrone by modification of a literature procedure, as summarized in Scheme 3.[9]

Dihydro (reduced) derivatives of 2,7-diOCH_3, 2,6-diH, and 2,6-diOCH_3 (abbreviated as r-2,7-diOCH_3, r-2,6-diH, and r-2,6-diOCH_3) were "captured" and isolated as stable acetates by reducing the corresponding dibromo-9,10-anthraquinone precursors with Zn in the presence

(5) Adachi, M.; Nagao, Y. *Chem. Mater.* **2001**, *13*, 662−669.

(6) Nepras, M,; Titz, M.; Gas, B.; Fabian, J. *Collect. Czech. Chem. Commun.* **1982**, *47*, 2594−2603. (b) Allen, N. S.; Pullen, G.; Shah, M.; Edge, M.; Holdsworth, D.; Catalina, F. *J. Photochem. Photobiol. A: Chem.* **1995**, *91*, 73−79. (c) Nakayama, T.; Torii, Y.; Nagahara, T.; Nagahara, T.; Miki, S.; Hamanoue, K. *J. Phys. Chem. A* **1999**, *103*, 1696−1703. (d) Inoue, H.; Hida, M.; Nakashima, N.; Yoshihara, K. *J. Phys. Chem.* **1982**, *86*, 3184−3188.

(7) Elder, I. A. Ph.D. Dissertation, University of Missouri−Rolla, Rolla, MO, 2001; pp 176, 191.

(8) Akiyama, S.; Nakatsuji, S.; Yoshida, K.; Nakashima, K.; Hagiwara, T.; Tsuruta, H.; Yoshida, T. *Bull. Chem. Soc. Jpn.* **1983**, *56*, 361−362. (b) Leonard, K. A.; Nelen, M. I.; Anderson, L. T.; Gibson, S. L.; Hilf, R.; Detty, M. R. *J. Med. Chem.* **1999**, *42*, 3942−3952.

(9) Perry, P. J.; Reszka, A. P.; Wood, A. A.; Read, M. A.; Gowan, S. M.; Dosanjh, H. S.; Trent, J. O.; Jenkins, T. C.; Kelland, L. R.; Neidle, S. *J. Med. Chem.* **1998**, *41*, 4873−4884. (b) Gubelmann, I.; Weiland, H. J.; Stallman, O. *J. Am. Chem. Soc.* **1931**, *53*, 1033−1036.

Table 1. Properties of 2,7-diX, 2-X, and 2,6-diX in Liquid CH_2Cl_2, in Frozen CH_2Cl_2, and as Solids

compound	abs max, nm (log ϵ)	σ_{p-X}[a]	$\lambda_{max,em}$, 298 K, nm	Stokes shift cm^{-1}	Stokes shift nm	Φ_{em}	$\lambda_{max,em}$ 77 K, nm	$\lambda_{max,em}$ 298 K, nm (solid)	$E_{1/2}$,[b] V	E_{HOMO}, eV	E_{LUMO}, eV	dipole moment (D)[c]	dihedral[d] (deg)
9,10-anthraquinone	253 (4.11), 271 (3.69), 321 (3.17)	–	none	–	–	–	–	–	−1.490 −1.837	−9.677	0.704	0.00	
2,7-diS$(CH_3)_2^+$	310 (4.23), 400 (3.70)	0.9	634	9227	234	<0.001	600	601		−12.451	−2.749		82.8
2,7-diNO_2	315 (4.72), 369 (4.45)	0.78	567	9484	198	0.002	576	590	*p*	−9.625	0.019	5.59	90
2,7-di$COCH_3$	305 (5.05), 380 (4.51)	0.5	487	5782	107	<0.001	540	590, 505	−1.289 −1.641	−8.703	0.217	1.41	45
2,7-diCH_2CN	263 (4.19), 298 (4.80), 383 (4.46)	0.18	494	5867	111	<0.001	534	470	*p*	−9.114	0.312	4.70	90
2,7-diH	273 (4.54), 297 (4.84), 386 (4.23)	0	502[e]	5986	116	0.019	562[f]	549[g]	−1.288 −1.681	−8.861	0.460	0.75	16.5
2,7-diCH_3	264 (4.34), 301 (4.62), 393 (4.06)	−0.14	529	6542	136	0.021	585	565	−1.291 −1.684	−8.558	0.512	1.36	90
2,7-diOCH_3	274 (4.49), 306 (4.84), 414 (4.19)	−0.27	600[h]	7488	186	0.013	607[i]	580[j]	−1.309 −1.722	−8.090	0.496	2.98	51
2,7-diSCH_3	313 (4.86), 418 (4.42)	−0.3	634	8151	216	0.020	607	604		−7.976	0.435	3.12	61.6
2,7-di$N(CH_3)_2$	274 (4.49), 329 (4.74), 370 (4.58), 482 (4.38)	−0.83	none	–	–	–	670[n]	750[o]	−1.280 −1.704	−7.466	0.752	6.15	8.3
2-NO_2	268 (4.59), 318 (4.59), 360 (4.45)	0.78	532	8981	172	<0.001	523	578	−1.304 −1.468 −1.808	−9.528	0.337	6.13	90
2-H	251 (4.25), 283 (4.40), 371 (3.81)	0	491	6588	120	<0.001	528	596	−1.310 −1.766	−8.859	0.575	0.60	90
2-CH_3	251 (4.53), 298 (4.61), 380 (4.08)	−0.14	539	7763	159	0.015	546	568	−1.320 −1.780	−8.564	0.602	1.18	90
2-OCH_3	254 (4.62), 297 (4.58), 396 (4.12)	−0.27	593	8389	197	0.024	573	575	−1.323 −1.792	−7.932	0.764	3.12	8.9
2,6-diH	296 (4.87), 327 (4.83), 366 (4.49)	0	498	7242	132	0.002	560	536	−1.273 −1.695	−8.870	0.467	0.00	90
2,6-diOCH_3	258 (4.19), 306 (4.45), 342 (4.26), 391 (4.01)	−0.27	604[k]	9019	213	0.014	573l	610[m]	*p*	−8.081	0.505	2.34	49.1
2,6-diSCH_3	276 (4.70), 315 (4.85), 345 (4.78), 396 (4.54)	−0.3	636	9529	240	0.017	571	613		−7.942	0.441	2.04	55.8

[a] All from ref 14a, except $\sigma_{p\text{-}SCH_3}$, which was taken from ref 14b. [b] Determined in CH_2Cl_2/0.1 M tetrabutylammonium perchlorate and reported as volts versus ferrocene used as internal reference. [c] Of the ground state. [d] Between the two aromatic rings across the triple bond. [e] Lifetime of 2,7-diH at 298 K, $\tau_{2,7-diH}^{298K}$ = <200 ps (73.3%), 1.01 ns (17.3%), and 3.84 ns (9.4%). [f] $\tau_{2,7-diH}^{77K}$ = 1.63 ns (32.3%), 4.26 ns (42.1%), and 12.19 ns (24.7%). [g] $\tau_{2,7-diH}^{solid,298K}$ = 206 ps (7.7%), 1.46 ns (27.4%), and 5.16 ns (64.9%). [h] Lifetime of 2,7-diOCH_3 at 298 K, $\tau_{2,7-diOCH_3}^{298K}$ = 1.67 ns (100%) [i] $\tau_{2,7-diOCH_3}^{77K}$ = 581 ps (11.3%), 3.49 ns (46.3%), and 10.92 ns (42.4%). [j] $\tau_{2,7-diOCH_3}^{solid,298K}$ = 575 ps (5.3%), 2.88 ns (45.4%), and 7.25 ns (49.3%). [k] Lifetime of 2,6-diOCH_3 at 298 K, $\tau_{2,6-diOCH_3}^{298K}$ = 1.71 ns (90.6%) and 3.51 ns (9.4%). [l] $\tau_{2,6-diOCH_3}^{77K}$ = 2.14 ns (7.8%), 7.46 ns (41.4%), and 18.78 ns (50.9%). [m] $\tau_{2,7-diOCH_3}^{solid,298K}$ = 3.50 ns (41.8%) and 6.39 ns (58.2%). [n] $\tau_{2,7-diN(CH_3)_2}^{77K}$ < 200 ps. [o] $\tau_{2,7-diN(CH_3)_2}^{solid,298K}$ < 200 ps (76.6%) and 774 ps (23.5%). [p] Poor solubility.

Scheme 3. Synthesis of 2,7-Diamino- and 2,7-Dibromo-9,10-anthraquinone

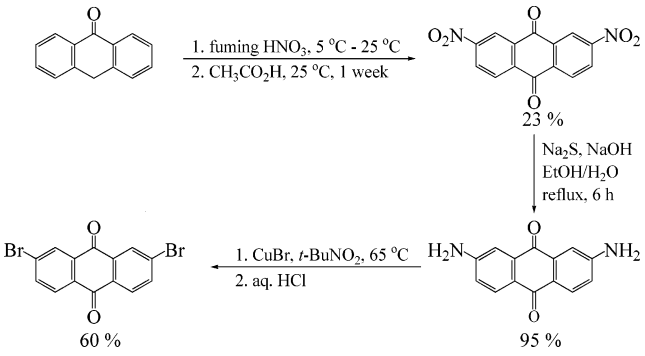

Scheme 4. Synthesis of the Reduced Form r-2,7-diOCH_3 of 2,7-diOCH_3[a]

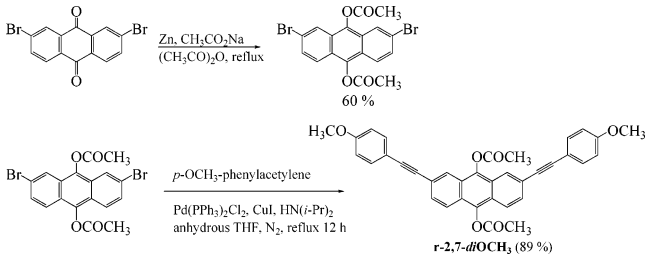

[a] r-2,6-diH and r-2,6-diOCH_3 were synthesized by analogous procedures.

of sodium acetate and acetic anhydride,[10] followed by Sonogashira coupling reactions with the corresponding phenylacetylenes (Scheme 4).

It is noted that with the exception of 2-H and 2-CH_3, all other compounds of this study are new molecules. Reported syntheses of 2-H include a Sonogashira coupling of 2-iodo-9,10-anthraquinone with phenylacetylene[11] and a pyrolytic process through a Wittig reaction intermediate obtained in analogy to the first step in Scheme 2.[12] 2-CH_3 has been made via the latter method only.[12] No photophysical, electrochemical, or structural data for these compounds have been reported.

2. Photophysical and Electrochemical Characterization of 2,7-diXs, 2,6-diXs, and 2-Xs, as Well as of Selected Reduced Forms. Most of the photophysical and redox studies were conducted in CH_2Cl_2 for two reasons. First, the poor solubility of 2,6-diXs and 2,7-diXs in most organic solvent limits the choice of a

(10) Power, G.; Hodge, P.; Clark, I. D.; Rabjohns, M. A.; Goodbody, I. *Chem. Commun.* **1998**, 873−874.

(11) Moroz, A. A.; Budzinskaya, I. A.; Mamedov, T. Z.; Galevskaya, T. P. *Zh. Org. Khim.* **1982**, *18*, 1472−1475.

(12) Listvan, V. N.; Stasyuk, A. P.; Kornilov, M. Yu.; Komarov, I. V. *Zh. Obshch. Khim.* **1990**, *60*, 804−807.

Table 2. Effect of Solvent on the Spectroscopic Properties of 2-OCH_3

solvent	dielectric constant[a] (ϵ_s)	refractive index[a] (n)	$\lambda_{max,abs}$, nm	$\lambda_{max,em}$ 298 K, nm	$\lambda_{max,em}$ 77 K, nm	Mataga parameter	Stokes shift at 298 K, nm (cm^{-1})	Φ_{em}[b]
benzene	2.28	1.5011	391	505	571	0.0026	114 (5773)	0.013
toluene	2.38	1.4961	391	502	478	0.0135	111 (5655)	0.006
$CHCl_3$	4.7	1.4459	398	567	513	0.1455	169 (7488)	0.059
CH_3COOEt	6.02	1.3723	386	562	501	0.1997	176 (8113)	0.037
CH_2Cl_2	8.9	1.4242	396	593	573	0.2165	197 (8389)	0.024
DMSO	49	1.4770	393	645	562	0.2645	252 (9941)	<0.005
CH_3CN	36.2	1.3441	384	647	561	0.3047	263 (10585)	<0.005

[a] From ref 15. [b] From ref 16.

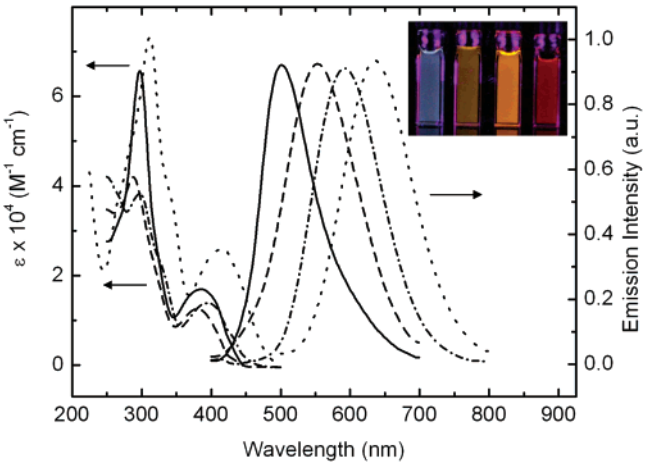

Figure 1. Comparative absorption and emission spectroscopy of four representative 2,7-diXs and 2-Xs: 2,7-diH (—), 2-CH_3 (– – –), 2-OCH_3 (·—·—·), and 2,7-diSCH_3 (···) in CH_2Cl_2. (Concentrations in the ~10^{-4} M range.) Inset: Photograph of the same solutions under ultraviolet light.

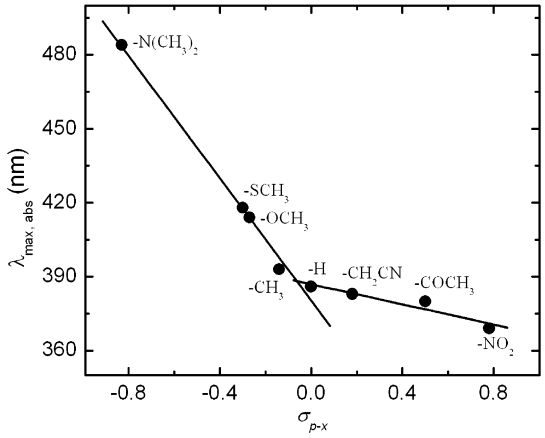

Figure 2. Relationship between the maximum absorption wavelength $\lambda_{max,abs}$ and the Hammett substituent constant σ_{p-X} for the 2,7-diXs.

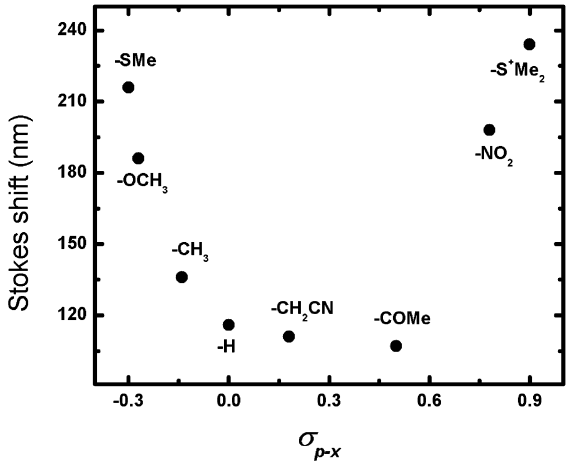

Figure 3. Relationship between the Stokes shift and the Hammett substituent constant σ_{p-X} for the 2,7-diXs.

common solvent for all compounds. Second, among all solvents considered, methylene chloride is one of the solvent in which we have observed stronger photoluminescence (vide infra, Table 2). Photophysical and electrochemical data for all 2,7-diXs, 2,6-diXs, and 2-Xs are summarized in Table 1. Figure 1 shows room-temperature electronic absorption and emission data of four representative substituted 9,10-anthraquinones (2,7-diH, 2-CH_3, 2-OCH_3, and 2,7-diSCH_3). It is noted that substitution has a smaller effect on the absorption spectra than it has on the emission spectra. Thus, Figure 2 shows that as substituents become more electron-donating (i.e., as the substituent constant, σ_{p-X}, decreases) the longest wavelength absorption maximum, $\lambda_{max,abs}$, increases monotonically (e.g., by 49 nm from 2,7-diNO_2 to 2,7-diSCH_3). However, the overall change is not linear: the curve changes slope suddenly when electron-donating substituents have delocalizable electron pairs [e.g., $-OCH_3$, $-SCH_3$, and $-N(CH_3)_2$]. On the other hand, the emission spectra are featureless, emission lifetimes are very short (see Table 1), and the emission quantum yields are ≤2.4%. The only derivative that is not photoluminescent in solution is 2,7-di$N(CH_3)_2$, probably due to charge-transfer bimolecular quenching by the amine.[13] The wavelength of maximum emission, $\lambda_{max,em}$, as a function of substitution does not vary monotonically as a function of substitution (Figure 3 and Table 1), and the Stokes shift can vary from as low as ~100 nm to as large as over 200 nm for both electron-donating and electron-withdrawing substituents. All other factors kept constant, $\lambda_{max,em}$ depends strongly on the solvent polarity. This is demonstrated with 2-OCH_3 in Table 2.

It is noted that for solubility reasons this study could not be done with any of the 2,6-diXs or the 2,7-diXs. Nevertheless, on the basis of the spectroscopic (vide ante), redox, and orbital (vide infra) similarities among 2,6-diXs, 2,7-diXs, and 2-Xs, the results obtained with 2-OCH_3 are considered general. Thus, while $\lambda_{max,abs}$ of that compound changes only from 391 to 384 nm by going from nonpolar benzene to polar acetonitrile, the value of $\lambda_{max,em}$ changes from 505 to 647 nm. The Stokes

(13) Ghosh, H. N.; Pal, H.; Palit, D. K.; Mukherjee, T.; Mittal, J. P. *J. Photochem. Photobiol. A: Chem.* **1993**, *73*, 17−22. (b) Gorner, H. *Photochem. Photobiol.* **2003**, *77*, 171−179. (c) Zallesskaya, G. A.; Yakovlev, D. L.; Sambor, E. G. *J. Appl. Spectrosc.* **2002**, *69*, 526−533.

shift (in cm^{-1}), that is the energy difference between (a) the equilibrium ground state and the Franck−Condon excited state and (b) the equilibrium excited state and the Franck−Condon ground state, shows a very good correlation (correlation coefficient = 0.98) with the Lippert−Mataga polarity parameter, $[(e_s - 1)/(2e_s + 1) - (n^2 - 1)/(2n^2 + 1)]$, according to eq 1,

$$\bar{\nu} = \text{constant} + \frac{1}{4\pi hc\epsilon_o}\frac{(\Delta\mu)^2}{\alpha^3}\left(\frac{\epsilon_s - 1}{2\epsilon_s + 1} - \frac{n^2 - 1}{2n^2 + 1}\right) \quad (1)$$

which quantifies the difference in polarization between the excited and the ground state of a molecule and allows estimation of the dipole moment of the excited state.[17] (In eq 1 $\bar{\nu}$ is the Stokes shift in wavenumbers, h is the Planck constant, c is the speed of light, ϵ_o is the permittivity of free space, $\Delta\mu$ is the change in dipole moment between the ground and excited states, α is the radius of the spherical cavity in the solvent occupied by the molecule, ϵ_s is the static dielectric constant and n the refractive index of the solvent.)

Another remarkable feature of arylethynyl-9,10-anthraquinones is a strong emission from solid samples. The value of $\lambda_{max,em}$ from solid samples can be longer or shorter than the corresponding $\lambda_{max,em}$ value in CH_2Cl_2, but the relative values vary consistently for the same substituents across the 2,7-diX, 2,6-diX, and 2-X groups of compounds. To rationalize the emission from the solid samples, we have investigated the crystal structure of 2,7-diH as a representative example of the compounds of this study (vide infra).

Upon electrochemical reduction, all 2,7-diX, 2,6-diX, and 2-Xs show a behavior analogous to that of 9,10-anthraquinone (see Figure 5), with two well-separated reduction waves, whose position is practically independent of substitution. This implies that the point of substitution and the point of reduction (i.e., the LUMO) are spatially far from one another.

The spectroscopic properties of stable reduced forms r-2,7-diOCH_3, r-2,6-diH, and r-2,6-diOCH_3 are distinctly different from those of the corresponding oxidized forms. Both the absorption and the emission spectra are significantly blue-shifted relative to those of the oxidized forms (Figure 6) and resemble the spectra of anthracene (Table 3) and of 9,10-dihydroxyanthracene.[18] None of these species demonstrates reversible electrochemistry.

3. Molecular Modeling of Phenylethynyl-Substituted 9,10-Anthraquinones. To rationalize the spectroscopic and electrochemical properties of 2,7-diXs, 2,6-diXs, 2-Xs, and their reduced forms, we conducted single point energy calculations on their PM3-optimized ground-state geometries. As representative examples, the resulting HOMOs and LUMOs of 2,7-diOCH_3, 2-OCH_3, and 2,7-diNO_2 are shown in comparison with the same orbitals of 9,10-anthraquinone in Figure 7. Generally, in molecules with delocalizable electron donors the anthraquinone core is puckered across the carbonyl/

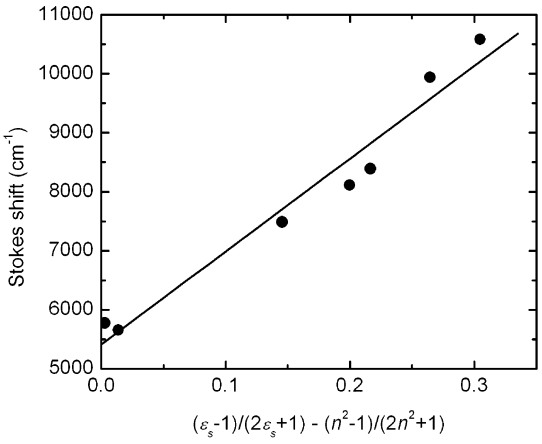

Figure 4. Correlation according to eq 1 of the Stokes shift ($\bar{\nu}$) and the Lippert−Mataga polarity parameter for 2-OCH_3 in the seven solvents listed in Table 2 (slope = 15 729 ± 1394 cm^{-1}; intercept = 5415 ± 274 cm^{-1}; R^2 = 0.980).

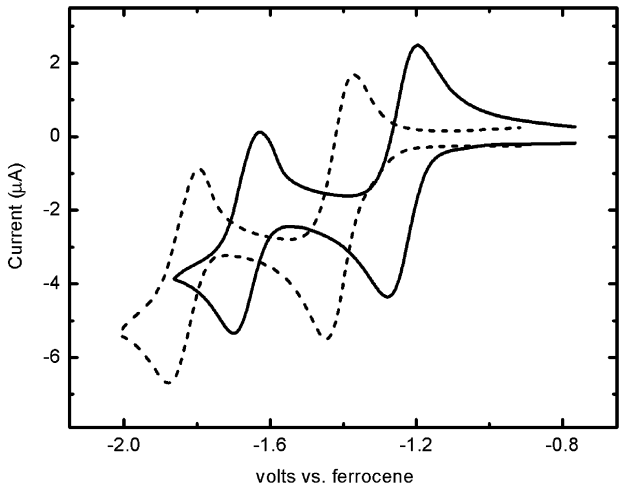

Figure 5. Comparative cyclic voltammetry at 0.1 V s^{-1} of 2,7-diH (—; 0.47 mM) and 9,10-anthraquinone (− − −; 0.52 mM) in Ar-degassed CH_2Cl_2/0.1 M TBAP solutions using a Au-disk electrode (0.0201 cm^2)

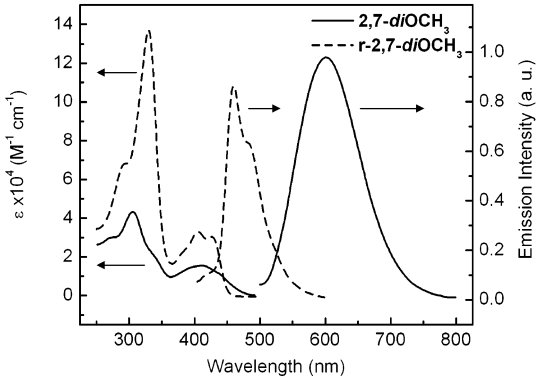

Figure 6. Comparative absorption and emission spectroscopy of 2,7-diOCH_3 and the reduced form *r*-2,7-diOCH_3 in dichloromethane. (Concentrations in the ~10^{-4} M range.)

(14) Isaacs, N. *Physical Organic Chemistry*, 2nd ed.; Longman Scientific and Technical: Essex, U.K. 1995; p 152. (b) Nguyen, P.; Yuan, Z.; Agocs, L.; Lesley, G.; Marder, T. B. *Inorg. Chim. Acta* **1994**, *220*, 289−296.

(15) Gordon, A. J.; Ford, R. A. *The Chemist's Companion: A Handbook of Practical Data, Techniques, and References*; Wiley & Sons: New York, 1972.

(16) Consistent with the energy gap law, generally the emission quantum yield decreases as the emission maximum moves to longer wavelengths.

(17) Würthner, F.; Ahmed, S.; Thalacker, C.; Debaerdemaeker, T. *Chem. Eur. J.* **2002**, *8*, 4742−4750. (b) Mertz, E. L.; Tikhomirov, V. A.; Krishtalik, L. I. *J. Phys. Chem. A* **1997**, *101*, 3433−3442. (c) Lippert, E.; Lüder, W. *Z. Physik. Chem. (Frankfurt)* **1962**, *1962*, 60−81. (d) Lippert, E. *Z. Elektrochem.* **1957**, *61*, 962−957. (e) Mataga, N.; Kaifu, Y.; Koizumi, M. *Bull. Chem. Soc. Jpn.* **1955**, *28*, 690−691. (f) Mataga, N.; Kaifu, Y.; Koizumi, M. *Bull. Chem. Soc. Jpn.* **1956**, *29*, 465−470.

(18) Carlson, S. A.; Hercules, D. M. *Anal. Chem.* **1973**, *45*, 1794−1799.

Table 3. Spectroscopic Data for Selected Reduced r-2,7-diX and r-2,6-diX Compounds in CH_2Cl_2

compound	$\lambda_{max,abs}$, nm ($\epsilon \times 10^{-4}$)	$\lambda_{max,em}$, nm 298 K	$\lambda_{max,em}$, nm 77 K	298 K (pure solid sample)	Φ
anthracene	374 (1.14), 355 (1.3), 328 (0.91), 323 (0.49)	436, 415, 415			0.3
r-2,7-diOCH$_3$	292 (6.39), 332 (13.8), 384 (1.96), 405 (3.06), 430 (2.91)	476, 457[a]	499, 530[b]	497, 523[c]	0.613
r-2,6-diH	310 (7.57), 321 (10.6), 380 (2.12), 401 (1.50), 423 (1.35)	468, 443	489		0.582
r-2,6-diOCH$_3$	265 (4.18), 298 (4.04), 346 (8.89), 376 (1.34), 398 (1.13)	467, 453[d]	477, 494 (sh)[e]	500, 530[f]	0.333

[a] Lifetime of r-2,7-diOCH$_3$ at 298 K, $\tau_{r-2,7-diOCH_3}^{298K} = 9.31$ ns (100%). [b] $\tau_{r-2,7-diOCH_3}^{77K} = 1.59$ ns (2.0%), 12.01 ns (36.0%), and 24.88 ns (63.0%). [c] $\tau_{r-2,7-diOCH_3}^{solid,298K} = 5.14$ ns (18.3%) and 15.47 ns (81.7%). [d] Lifetime of r-2,6-diOCH$_3$ at 298 K, $\tau_{r-2,6-diOCH_3}^{298K} = 2.80$ ns (99.0%) and 16.61 ns (1.0%). [e] $\tau_{r-2,6-diOCH_3}^{77K} = 2.22$ ns (52.1%) and 3.66 ns (47.9%). [f] $\tau_{r-2,6-diOCH_3}^{solid,298K} = 199$ ps (41.8%), 7.48 ps (47.6%), and 2.93 ns (19.8%).

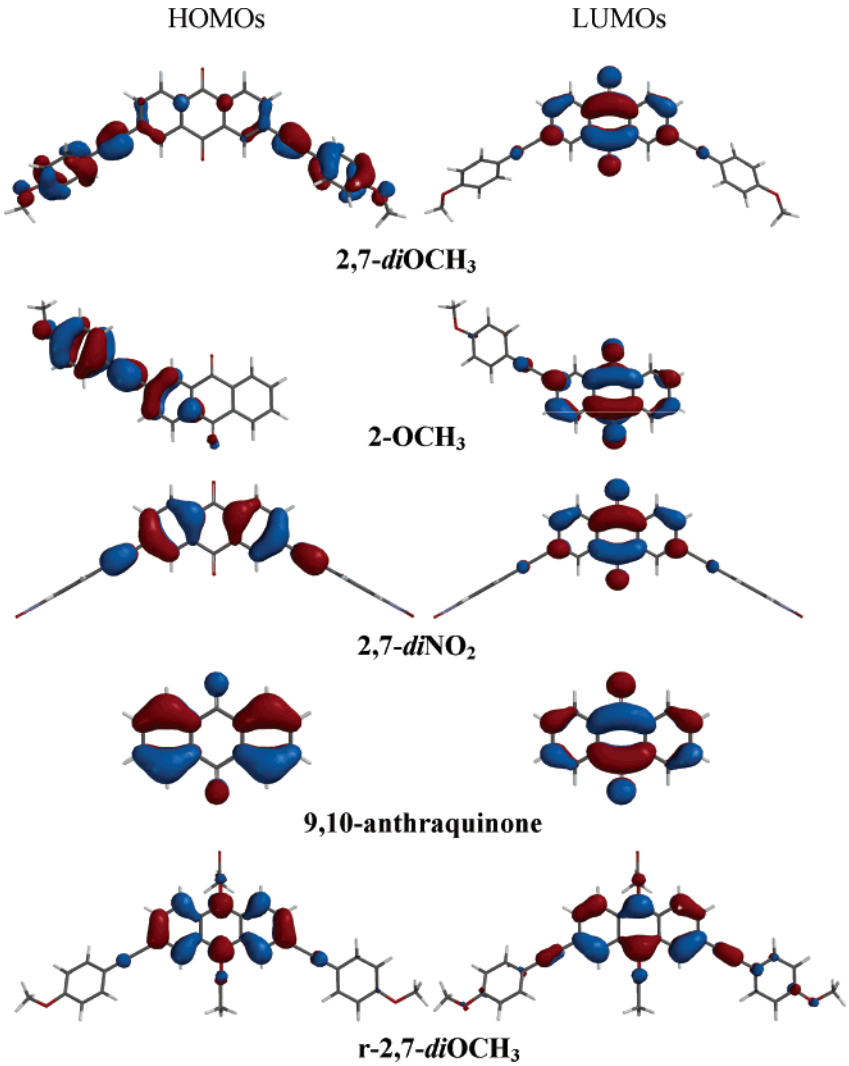

Figure 7. HOMO and LUMO of 2,7-diOCH$_3$, 2-OCH$_3$, 2,7-diNO$_2$, 9,10-anthraquinone, and the reduced form r-2,7-diOCH$_3$ according to ab initio calculations (3-21G(*) basis set) on PM3-optimized geometries.

carbonyl axis with a dihedral angle of 156°. In all cases the HOMOs extend mostly across the branches while all LUMOs are practically identical to the LUMO of 9,-10-anthraquinone and are "localized" over the core.[19] The calculated energies of these orbitals for all compounds, the corresponding ground state dipole moments, and the dihedral angles between the two aromatic rings across the triple bonds are included in Table 1. By comparing the relative energies of the HOMO and the LUMO, we see that they are approximately equal among corresponding mono- and disubstituted compounds, indicating that branches are practically isolated from one another. Ground-state dipole moments reflect the molecular geometry; they are nonzero even for "symmetric" 2,6-diXs, which appear puckered across the carbonyl/carbonyl axis.

By the same approach, the 9,10-anthraquinone core of reduced compounds is planar and all HOMOs and LUMOs are localized at the core. For comparison, the orbitals of r-2,7-diOCH$_3$ are also included in Figure 7.

Equilibrium geometries were also calculated for the first singlet excited state of 2-NO$_2$, 2-H, and 2-OCH$_3$ using configurational interactions with the 6-31G* basis set. (Larger molecules could not be handled, at least

(19) Although unusual, the situation where the HOMO and LUMO of quinone-type molecules are located at different parts of the molecule has been reported before. For example, see: Adachi, M.; Murata, Y. *J. Phys. Chem. A* **1998**, *102*, 841−845.

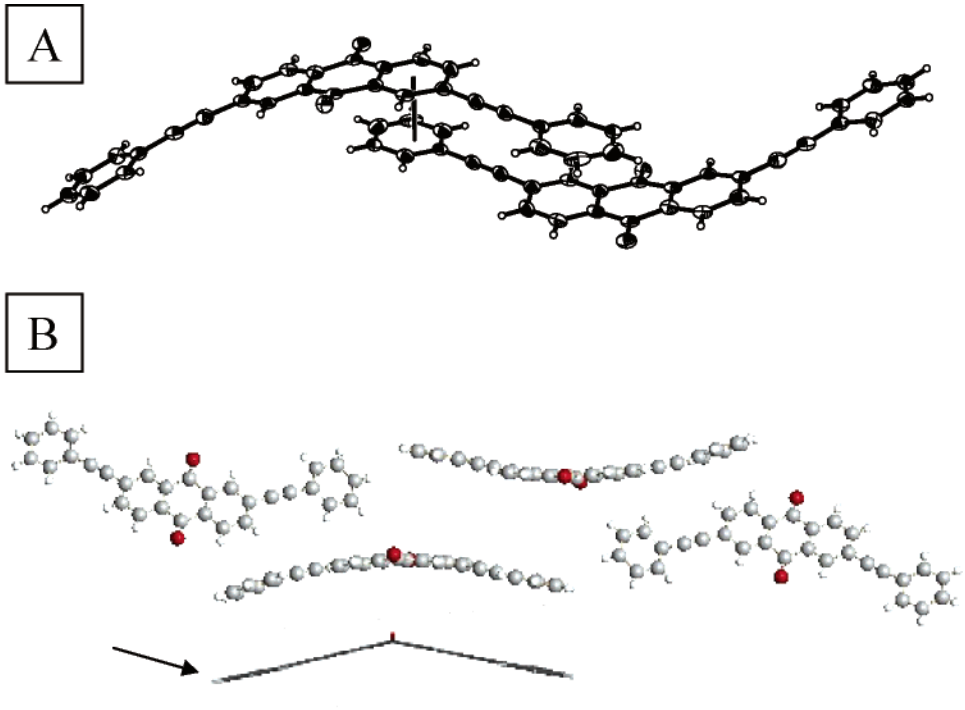

Figure 8. Results from X-ray analysis of 2,7-diH. (A) The molecule is bent and packs in a slipped-stack arrangement. The distance indicated by the bar is 4.02 Å. (B) Unit cell. Arrow shows the PM3-optimized structure.

time-wise.) The results are given as Supporting Information (Appendix II). The dihedral angle across the triple bond in 2-NO_2 and 2-H is still 90°. However, in 2-OCH_3, whose ground state is puckered across the carbonyl/carbonyl axis with a dihedral angle across the triple bond equal to 8.9°, the excited state is perfectly flat all across.

4. X-ray Analysis of 2,7-diH. The emission from solid samples is related not only to the molecular geometry but also to the crystal structure (see Discussion). We have been able to grow crystals of 2,7-diH suitable for X-ray analysis, and the results are illustrated in Figure 8. The crystal is monoclinic (space group $P2_1/n$) and the molecules pack in a slipped-stacked arrangement with a distance of 4.02 Å between the centroid of one of the aromatic rings of anthraquinone and the centroid of an aryl ring on an adjacent molecule. However, the most intriguing feature of this molecule is that it is bent. The dihedral angle of the aromatic rings of anthraquinone from the central ring range from 6.1° to 6.4°. Also, the dihedral angle from the central ring of the anthraquinone core to the terminal aryl rings range from 11.9° to 18.2°, producing an overall bend, in excellent agreement with the calculated bend (156°). The bond angles of the acetylenes deviate significantly from 180°. Bond angles between the aromatic ring of anthraquinone and the ethynyl group range from 175.9° to 176.7°, and between the ethynyl group and the terminal aryl groups range from 177.6° to 178.4°.

Discussion

Compounds 2,7-diX, 2,6-diX, and 2-X have three potentially useful properties: (a) very large Stokes shifts (100−250 nm), (b) emission from the solid state, and (c) very large differences in the emission spectra between oxidized and reduced forms (up to 130 nm). Understanding the cause for the large Stokes shifts may provide clues for the design of emitters in the near-infrared based either on this class of compounds or employing the same pattern of substitution. Emission from the solid state may be also a useful property for luminescent displays, while the wide difference in the emission spectrum from the oxidized and the reduced forms points to novel optoelectronic systems based on an *electrochromoluminescent* effect, i.e., electrochemical modulation of the emission spectrum in analogy to the well-known electrochromic effect, which refers to the electrochemical modulation of the absorption spectrum.[20]

With regard to the Stokes shifts, there are two phenomena to account for: (a) the overall large Stokes shift observed with all the compounds of this study and (b) particularly the larger Stokes shifts observed with both electron-donating and -withdrawing substituents (Figure 3). Large Stokes shifts might be attributed to eximer emission, to phosphorescence, to a large conformational change between the Franck−Condon and the emitting state, or to a large solvent reorganization after photoexcitation. In the case of 2,7-diXs, 2,6-diXs, and 2-Xs, the short-lived rather featureless fluid solution photoemission is concentration-independent and generally different from the emission at 77 K; thus, it is not assigned to eximer emission or phosphorescence. Furthermore, calculated excited-state geometries for 2-H, 2-NO_2, and 2-OCH_3 show no significant change from their respective ground states: the dihedral in 2-H and 2-NO_2 remains at 90°, while 2-OCH_3 undergoes a small change from its slightly twisted ground state (8.9°) to a perfectly flat excited state. On the other hand, the similar photophysical, redox, and calculated ground-

(20) Leventis, N. Electrochromic Devices. In *Encyclopedia of Science and Technology*, 8th ed.; McGraw-Hill Book Co.: New York, 1997; Vol. 6, p 153−156.

state structural properties of 2,7-diXs, 2,6-diXs, and 2-Xs (Table 1) allow us to reason by analogy for all 2,7-diXs and 2,6-diXs and conclude that possibilities for increased delocalization in the excited state through "gross" geometric reorganization, as in the classic case of biphenyl or of 2,2′-bipyridine,[21] should be ruled out.[22] The remaining factor that would produce a very large Stokes shift is solvent reorganization around the excited-state dipole. This conclusion is supported by both the relative distribution in space of the HOMO and LUMO (Figure 7) and the good correlation of the Stokes shift with the polarization of the medium according to eq 1 (Figure 4). Thus, modeling shows a mostly branch-located HOMO and a core-localized LUMO. Indeed, the similarity in the photophysical properties of 2,7-diXs, 2,6-diXs, and 2-Xs confirms that branches are more or less independent from one another, and the almost complete insensitivity of all redox potentials ($E_{1/2}$) to substitution supports that the LUMO is core-localized. The different spatial distribution of the HOMO and the LUMO leads to orbital-overlap, unfavorable transitions, and low emission quantum yields.[23] The fact that photoexcitation leads to a large dipole is confirmed by analysis of the slope (=15 729 cm^{-1}) of the Lippert−Mataga plot for 2-OCH_3, shown in Figure 4. According to eq 1, this slope is equal to $(\Delta\mu)^2/(4hc\pi\epsilon_o\alpha^3)$. It follows from modeling of 2-OCH_3 that $\alpha \approx 9.121$ Å (equal to half of the longest molecular dimension: 18.242 Å). Thus $\Delta\mu = 1.62 \times 10^{-28}$ C m (or 48.56 D). The calculated ground-state dipole moment of 2-OCH_3 is 3.12 D (Table 1). Therefore, the excited-state dipole moment should be ∼52 D. As was stated above, stabilization through solvation of this large dipole leads to significant solvent reorganization and results in large Stokes shifts.

Now, as the electron-donating ability of the substituents increases, the energy of the HOMO rises, rendering the HOMO−LUMO gap narrower and shifting the absorption $\lambda_{max,abs}$ to longer wavelengths (Figure 2). The most striking feature of Figure 2, however, is the sudden change in the slope:[24] this is attributed to resonance interactions developing between, for example, the n-electrons of the $-OCH_3$ group and the HOMO, in analogy to similar changes in the slope of Hammett "linear" free energy relationships for certain classes of chemical reactions.[25] This resonance participation of the n-electrons of the substituent is clearly indicated by the results of molecular modeling for 2,7-diOCH_3 (Figure 7 and Table 1). Thus, the results of Figure 2, taken together with Figure 7 and the E_{HOMO} values of Table 1, support the view that adding electron density in the HOMO by resonance raises the energy of the ground-state, accounting for the larger Stokes shifts observed with electron-donating substituents. On the other hand, electron-withdrawing substituents delocalize the LUMO, lower its energy (Table 1), and account for the observed increase in the Stokes shifts with electron-withdrawing substituents.

Solid samples of 2,7-diX, 2,6-diX, and 2-Xs are also photoluminescent, and the photoemission may be blue- or red-shifted relative to the emission in solution.[26] This wavelength shift depends on the substituents and remains consistent in the three groups of compounds. In general, the fact that aryethynyl-substituted 9,10-anthraquinones are photoluminescent is related to the crystal structure of the solids. Thus, from the unit cell of 2,7-diH (Figure 8) we see that although the substituted 9,10-anthraquinone moieties are arranged parallel and only 4.02 Å apart from one another, they are nevertheless also offset so that only the terminal aryl ring and only one of the aromatic 9,10-anthraquinone rings of two neighboring molecules are superimposed in space. Since the LUMO is localized at the anthraquinone core and because there is no spatial orbital overlap between adjacent anthraquinone cores in the crystal, there is little chance for electron hopping between neighboring sites promoting radiationless deactivation.

Finally, the dramatic change in the photoluminescence spectrum upon chemical reduction is again attributed to the relative HOMO/LUMO location. Now, both the HOMO and the LUMO of the reduced form are located on the disubstituted dihydro-9,10-anthraquinone, whose photophysical properties resemble those of anthracene. The transitions are all orbital-overlap-allowed, leading to relatively high emission quantum yields (Table 3).

Conclusions

Several arylethynyl-substituted 9,10-anthraquinones have been synthesized, and it has been shown that they are photoluminescent both in solution and as solids. Our results emphasize the fact that in the quest for materials with longer emission wavelengths, not only extending the conjugation but also dipole moment changes should be considered. In this regard, arylethynyl substitution is an effective tool. Thus, the emission of the title compounds could be shifted farther toward the near infrared by not only extending the conjugation along the branches (for example, by introducing bisethynyl bridges between the antraquinone core and the aryl groups) but also by forcing even larger dipole moment changes by asymmetric substitution. For example, modeling shows that the 2,7-OCH_3,NO_2 analogue would have a $-OCH_3$

(21) Wagner, P. J. *J. Am. Chem. Soc.* **1967**, *89*, 2820−2825. (b) Leventis, N.; Ph.D. Dissertation, Michigan State University, East Lansing, MI, 1985; p 53.

(22) By the same token, if the dihedral across the triple bond is forced flat, as in the case of 2,7-diH in the crystal (Figure 8), a more extended π-delocalization may explain the red-shifted emission (by 47 nm; see Table 1) relative to the emission in solution. (Similar phenomena may prevail in frozen matrixes at 77 K.)

(23) A second more subtle effect is the variation of the quantum yields with substitution: electron donors tend to give compounds with higher quantum yields than electron acceptors. One possible reason may be related to the relative magnitude of the dipole moment change as reflected in the transition moment. Thus, it is noted, for example, that the spatial HOMO−LUMO separation in 2,7-diNO_2 (Figure 7) is not as large as in 2,7-diOCH_3.

(24) Changes in the slope of $\lambda_{max,abs}$ as a function of substitution have been reported before for other classes of compounds as well. For example, it has been reported, but not elaborated, that both electron-donating and electron-withdrawing groups may exert a bathochromic shift in certain bis(*p*-X-phenylethynyl)benzenes and 9,10-bis(*p*-X-phenylethynyl)anthracenes (Nakatsuji, S.; Matsuda, K.; Uesugi, Y.; Nakashima, K.; Akiyama, S.; Fabian, W. *J. Chem. Soc., Perkin Trans. 1* **1992**, 755−758).

(25) See, for example: Um, I.-H.; Han, H.-J.; Ahn, J.-A.; Kang, S.; Buncel, E. *J. Org. Chem.* **2002**, *67*, 8475−8480.

(26) Weak room-temperature photoemission from certain solid 9,-10-anthraquinone derivatives has been reported before (for example, see: Breslin, D. T.; Fox, M. A. *Chem. Phys. Lett.* **1995**, *239*, 299−305); slower internal conversion has been attributed to the restricted motion of the side chains. The possible role of orbital overlap on the deactivation of the excited state was not discussed.

branch localized HOMO and a $-NO_2$ branch localized LUMO. Clearly, in this case the induced charge separation, exited state dipole moment, and bathochromic shift will all be larger than those of 2,7-diOCH_3 or 2,7-diNO_2. Finally, the quite different photoluminescent properties among the arylethynyl-substituted 9,10-anthraquinones and the corresponding dihydro-9,10-anthraquinones indicates that if this transition is carried out reversibly (e.g., by electrochemical means), it will potentially lead to a new class of optoelectrochemical systems for switches, sensors, and displays.

Experimental Section

Methods. All reactions with air- and/or moisture-sensitive compounds were performed under nitrogen in flame- or oven-dried glassware. Absorption spectra were obtained with a Bechman DU-640B spectrophotometer. Emission spectra were obtained with freeze−pump−thaw degassed samples using a system composed of an ORIEL pulsed N_2 laser model 79111 (5 ns), an ORIEL dye laser module model 79120 adjusted at 425 nm (Oriel Dye No. 79151) or at 370 nm (Oriel Dye No. 79150), an ORIEL spectrograph model 77480, an InstaSpecV image intensifier/CCD detector, and a Stanford Research Systems, Inc. four-channel delay/pulse generator model DG535. Quasi-"steady-state" emission spectra were recorded with the same apparatus by setting the delay time to 700 ns and the gate width to 2000 ns. Low-temperature emission data were obtained by immersing NMR tubes containing the samples into a homemade vacuum-sealed glass dewar filled with liquid N_2 (77 K). Luminescence lifetimes were measured with an IBH time-correlated single photon counting (TCSPC) system equipped with a IBH model TBX-04 photon detection module, an IBH NanoLED (403 nm, 1 MHz repetition, model 07) excitation source, and IBH FMAS DAS6 fluorescence decay analysis software. TCSPC detection was collected at peak emission through a 450 nm long pass filter until 10 000 counts were measured. Cyclic voltammetry was carried out with a EG&G 263A potentiostat controlled by the EG&G model 270/250 Research Electrochemistry Software 4.30. Gold disk working electrodes (1.6 mm diameter, 0.0201 cm^2) and Ag/AgCl/aqueous KCl (3 M) reference electrodes were purchased from Bioanalytical Systems, Inc. A Au foil (Aldrich) was employed as a counter electrode. ^1H and ^{13}C NMR spectra were recorded on a Varian INOVA 400 NMR spectrometer and are reported as parts per million (ppm) from TMS (δ). Infrared spectra were recorded on a Nicolet Magna-IR model 750 spectrometer. Melting points were uncorrected. Elemental analyses were performed by Prevalere Research Services, Inc., Whiteboro, NY.

Emission quantum yields at room temperature (Φ) were determined by using a Perkin-Elmer LS50B luminescence spectrometer with samples in freeze−pump−thaw degassed and flame-sealed ampules. Values are calculated according to $\Phi = \Phi_{std}(I_{unk}/I_{std})(A_{unk}/A_{std})(\eta_{unk}/\eta_{std})^2$, where Φ_{std} is the quantum yield of the standard (perylene in cyclohexane, $\Phi_{std} = 0.58 \pm 0.01$[27]). I_{unk} and I_{std} are the integrated emission intensities of the sample and the standard, respectively. A_{unk} and A_{std} are the absorbances of the sample and the standard at the excitation wavelength, and η_{unk} and η_{std} are the refractive indexes of the corresponding solutions (pure solvents were assumed).

For X-ray crystal structure analysis, crystals of 2,7-diH suitable for single-crystal X-ray diffraction studies were grown from a concentrated solution in CH_2Cl_2/benzene. Data sets were collected on a Bruker Apex CCD diffractometer with graphite-monochromated Mo Kα radiation ($\lambda = 0.71073$ Å). Unit cell determination was achieved by using reflections from three different orientations. Structure solution, refinement, and modeling were accomplished using the Bruker SHELXTL package.[28] The structure was obtained by full-matrix least-squares refinement of F^2 and the selection of appropriate atoms from the generated difference map. Supplementary crystallographic data has been deposited in the Cambridge Crystallographic Centre (deposition number: CCDC 233733). The data can be obtained free of charge via http://www.ccdc.cam.ac.uk/cgi-bin/catreq.cgi or from Cambridge Crystallographic Centre, 12 Union Road, Cambridge CB2 1EZ, UK, +44 1223 336408. X-ray crystal structure analysis of 2,7-diH: formula $C_{30}H_{16}O_2$, $M_w = 408.43$, yellow crystal 0.40 × 0.05 × 0.02 mm, $a = 5.680(2)$ Å, $b = 7.917(3)$ Å, $c = 44.94(2)$ Å, $\alpha = 90°$, $\beta = 90.802(7)°$, $\gamma = 90°$, $V = 2020.9(12)$ Å^3, $D_{calc} = 1.342$ Mg m^{-3}, $\mu = 0.083$ mm^{-1}, $Z = 4$, monoclinic, space group $P2_1/n$ (No. 14), $\lambda = 0.710\,73$Å, $T = 100$ K, ω and ϕ scans, 14 386 reflections collected, 3566 independent (R_{int} 0.0888), 289 refined parameters, R1/*w*R2 ($I \geq 2\sigma(I)$) = 0.0894/0.2558 and R1/wR2 (all data) = 0.1314/0.2797, maximum (minimum) residual electron density 0.345 (−0.349) e Å^{-3}, all hydrogen atoms were calculated and refined as riding atoms.

Molecular modeling was conducted using Spartan 02 (Wavefunction, Inc.) on a Compaq computer Model Evo N180. Single point energy calculations were conducted using the 3-21G(*) basis set on PM3 geometry-optimized structures. Excited-state equilibrium geometries for 2-NO_2, 2-H, and 2-OCH_3 were conducted using configurational interactions and the 6-31G* basis set.

Materials. P(*t*-Bu)$_3$ was purchased from Strem Chemicals. All other starting materials, reagents, and solvents were purchased from Aldrich or Acros and were used as received unless otherwise noted. Diisopropylamine was distilled from NaOH.

***p*-Ethynylacetophenone.** $Pd(PhCN)_2Cl_2$ (460 mg, 1.2 mmol) and CuI (152 mg, 0.8 mmol) were added to a flame-dried, round-bottom flask, which was then septum-capped and purged with nitrogen. Anhydrous dioxane (15 mL), P(*t*-Bu)$_3$ (6.25 mL, 10% solution in hexane), HN(*i*-Pr)$_2$ (15 mL), and 4-bromoacetophenone (10 g, 50 mmol) in 20 mL of dioxane were added sequentially with a syringe to the stirred reaction mixture. Finally, trimethylsilylacetylene (12 mL, 85 mmol) was also added to the flask. In a few minutes, a precipitate was formed. The reaction mixture was stirred at room temperature for 2 h. Subsequently, all solvents were removed under reduced pressure. The solid residue was triturated with hexane and the mixture was filtered through a short silica gel column eluted with hexane. Hexane was removed under reduced pressure and the product was further purified by vacuum distillation (0.8 Torr, 110 °C) to give an oily substance, which, upon cooling, solidified: yield 9.6 g (88%); mp 37−38 °C (lit.[29] mp 36−37 °C, lit.[30] mp 36 °C); ^1H NMR (400 MHz, $CDCl_3$) δ 7.89 (d, $J = 8.79$ Hz, 2H), 7.54 (d, $J = 8.79$ Hz, 2H), 2.59 (s, 3H), 0.27 (s, 9H); ^{13}C NMR (100 MHz, $CDCl_3$) δ 197.197, 136.336, 132.017, 128.063, 127.949, 103.966, 98.038, 26.552, −0.217; IR (KBr) 2999, 2966, 2899, 2153, 1690, 1609, 1414, 1360, 1266, 1246, 1179, 1018, 964, 884, 843, 769, 642, 588 cm^{-1}.

The above product was dissolved in methanol (50 mL), a catalytic amount of NaOH was added (0.1 g), and the mixture was stirred at room temperature for 0.5 h. Water was then added, and the precipitate was collected and washed with water. The product was further purified by vacuum sublimation at 50 °C: yield 5.37 g (84%); mp 67 °C (lit.[31] mp 69−70 °C); ^1H NMR (400 MHz, $CDCl_3$) δ 7.91 (d, $J = 8.52$ Hz, 2H), 7.57 (d, $J = 8.52$ Hz, 2H), 3.26 (s, 1H), 2.60 (s, 3H); ^{13}C NMR (100 MHz, $CDCl_3$) δ 197.166, 136.707, 132.222, 128.116, 126.841, 82.692, 80.339, 26.559; IR (KBr) 3214, 2113, 1690, 102, 1421, 1360, 1273, 1179, 1112, 1018, 957, 863, 837, 756, 689, 655, 588, 554 cm^{-1}.

(27) Dawson, W. R.; Windsor, M. W. *J. Phys. Chem.* **1968**, *72*, 3251−3260.

(28) Sheldrick, G. M. *SHELX97: Programs for Crystal Structural Analysis*; University of Göttingen, Göttingen, Germany 1997.

(29) Takahashhi, S.; Kuroyama, Y.; Sonogashira, K.; Higihara, N. *Synthesis* **1980**, 627−630.

(30) Thorand, S.; Krause, N. *J. Org. Chem.* **1998**, *63*, 8551−8553.

(31) Takahashi, S.; Kuroyama, Y.; Sonogashira, K.; Hagihara, N. *Synthesis* **1980**, *8*, 627−630.

***p*-Ethynylnitrobenzene** was synthesized from 4-bromonitrobenzene (4 g, 19.8 mmol) through a procedure that is analogous to the preparation of *p*-ethynylacetophenone. The reaction mixture was allowed to react for 12 h. After solvents were removed, the precipitate was triturated with CH_2Cl_2. The mixture was filtered through a short silica gel pad eluting with CH_2Cl_2. The solvents were removed under reduced pressure, and the solid was chromatographed on silica gel, eluting with CH_2Cl_2: ^{1}H NMR (400 MHz, $CDCl_3$) δ 8.15 (d, 2H), 7.58 (d, 2H), 0.26 (s, 9H). All of the product was dissolved in a mixture of CH_2Cl_2 and methanol (50 mL, 1:1, v/v), a catalytic amount of NaOH was added (0.1 g), and the mixture was stirred at room temperature for 0.5 h. The product was chromatographed on a silica gel column, eluting with CH_2Cl_2: yield 1.9 g (66%); mp 149−151 °C (lit.[32] mp 150−152 °C); ^{1}H NMR (400 MHz, $CDCl_3$) δ 8.21 (d, 2H), 7.65 (d, 2H), 3.36 (s, 1H); ^{13}C NMR (100 MHz, $CDCl_3$) δ 147.515, 132.935, 128.890, 123.532, 82.298, 81.577; IR (KBr) 3254, 3113, 2113, 1602, 1508, 1347, 1112, 850, 756, 682 cm^{-1}.

***p*-(Cyanomethyl)phenylacetylene** was synthesized from 4-bromopenylacetonitrile (4 g, 20.4 mmol) through an analogous procedure to the one used in the preparation of *p*-ethynylacetophenone. Chromatography under the same conditions did not separate the product from unreacted 4-bromopenylacetonitrile, so in the subsequent reaction for the synthesis of 2,7-diCH_2CN we used the crude mixture.

***p*-(Dimethylamino)phenylacetylene.** A hexane solution of *n*-BuLi (1.6 M, 6.3 mL, 10 mmol) was added to a suspension of (chloromethyl)triphenylphosphonium chloride (3.57 g, 10 mmol) in THF (20 mL) cooled in an ice−water bath. The mixture was stirred for 30 min and powdered *p*-(dimethylamino)benzaldehyde (1.04 g, 7 mmol) was added to the resulting orange red solution of (chloromethylene)triphenylphosphorane. The new mixture was stirred at room temperature overnight. The residue obtained by evaporation of the solvent was extracted with heptane (300 mL). The heptane solution was passed through a short column of silica gel (5 g) and concentrated to a light yellow solid (1.02 g, 80%). The product is a mixture of cis- and trans-isomers (cis:trans ∼ 2:1) of *p*-(dimethylamino)-*β*-chlorostyrene: ^{1}H NMR (400 MHz, $CDCl_3$) δ cis, 7.63 (d, J = 9.13 Hz, 2H), 6.70 (d, J = 9.13 Hz, 2H), 6.50 (d, J = 8.09 Hz, 1H), 6.03 (d, J = 8.09 Hz, 1H), 2.952 (s, 6H); trans, 7.18 (d, J = 8.97 Hz, 2H), 6.75 (d, J = 13.48, 1H), 6.66 (d, J = 8.97 Hz, 2H), 6.42 (d, J = 13.48, 1H), 2.984 (s, 6H). To a solution of this product (2 g, 11 mmol) in THF (20 mL) was added *n*-BuLi in hexane (18.75 mL, 1.6 M, 30 mmol) under N_2 at −20 °C. The mixture was stirred for 2 h and then quenched with water. The aqueous layer was extracted with hexane (100 mL). The organic layers were combined, washed with water, dried over anhydrous $MgSO_4$, and evaporated to dryness to give *p*-(dimethylamino)phenylacetylene: yield 1.53 g (96%); mp 37−39 °C (lit.[8a] mp 50−52 °C; lit.[8b] mp 33−35 °C); ^{1}H NMR (400 MHz, $CDCl_3$) δ 7.37 (d, J = 8.98 Hz, 2H), 6.61 (d, J = 8.98 Hz, 2H), 3.00 (s, 1H), 2.97 (s, 6H); ^{13}C NMR (100 MHz, $CDCl_3$) δ 150.369, 133.178, 111.654, 108.740, 84.832, 74.38; IR (KBr) 3268, 2905, 2818, 2093, 1622, 1522, 1448, 1367, 1166, 1065, 951, 823, 675, 601 cm^{-1}.

2,7-Dinitro-9,10-anthraquinone. Anthrone (5 g, 26 mmol) was added slowly with stirring to fuming nitric acid (40 mL) at 5 °C. Subsequently, 100 mL of glacial acetic acid was added to the reaction mixture with cooling. The resulting solution was allowed to stand at room temperature for 1 week. At the end of the period, the yellow precipitate was collected by filtration, washed with acetic acid (3 × 10 mL) and hexane (3 × 10 mL), and dried under vacuum. The crude product was recrystallized from nitrobenzene/glacial acetic acid (1:1 v/v): yield, 1.25 g of pale yellow flaky crystals (16%); mp 290−291 °C (lit.[9a] mp 290−291 °C); ^{1}H NMR (400 MHz, DMSO) δ 8.84 (d, J = 2.38 Hz, 2H), 8.69 (dd, J = 2.38 Hz, J = 8.61 Hz, 2H), 8.48 (d, J = 8.61 Hz, 2H).

2,7-Diamino-9,10-anthraquinone. An aqueous solution (50 mL) of $Na_2S{\cdot}9H_2O$ (2.8 g, 12 mmol) and NaOH (1.1 g, 28 mmol) was added to a stirred suspension of 2,7-dinitroanthrance-9,10-dione (0.75 g, 2.5 mmol) in ethanol (40 mL). The mixture was refluxed for 6 h and allowed to stand overnight. Ethanol was removed by rotary evaporation. The resulting precipitate was collected and washed with water. Recrystallization from ethanol/water (3:1 v/v) afforded an orange/red solid: yield 0.56 g (95%); mp 337−339 °C (lit.[9a] mp 337−338 °C, lit.[9b] mp 330−332 °C); ^{1}H NMR (400 MHz, DMSO) δ 6.38 (4H, d, NH_2), 6.88 (2H, dd, J = 8.4 Hz, J = 2.3 Hz), 7.22 (2H, d, J = 2.4 Hz), 7.83 (2H, d, J = 8.4 Hz); ^{13}C NMR (100 MHz, DMSO) δ 184.225, 179.231, 153.617, 134.825, 128.860, 121.892, 117.908, 109.536.

2,7-Dibromo-9,10-anthraquinone. Anhydrous copper(II) bromide (6.8 g, 30.5 mmol), *tert*-butyl nitrite (4.3 mL, 36 mmol), and anhydrous acetonitrile (150 mL) were added to a three-neck round-bottom flask, and the mixture was heated to 65 °C. 2,7-Diamino-9,10-anthraquinone (2.9 g, 12 mmol) was added slowly over a period of 5 min to the reaction mixture. Nitrogen was evolving during the reaction. After nitrogen evolution had subsided, the reaction mixture was cooled to room temperature and poured into an aqueous HCl solution (100 mL, 20% w/v). The crude solid product was collected, washed with ether, and chromatographed on a silica gel column, eluting with hexane/CH_2Cl_2 (1:1, v/v) to afford a pale yellow solid: yield 2.6 g (60%); mp 248−250 °C; ^{1}H NMR (400 MHz, $CDCl_3$) δ 8.44 (d, J = 2.02 Hz, 2H), 8.18 (d, J = 8.24 Hz, 2H), 7.95 (dd, J = 2.02 Hz, J = 8.24 Hz, 2H); ^{13}C NMR (100 MHz, $CDCl_3$) δ 181.634, 180.959, 137.524, 134.184, 131.892, 130.382, 130.025, 129.122; IR (KBr) 3080, 3026, 1683, 1582, 1327, 1287, 931, 870, 729, 689, 649 cm^{-1}.

General Procedure for the Synthesis of 2,7-Bis(4-arylethynyl)-9,10-anthraquinones. 2,7-Dibromoanthraquinone (0.8 mmol), 4-substituted phenylacetylene (2.0 mmol), $Pd(PPh_3)_2Cl_2$ (0.08 mmol), and CuI (0.08 mmol) were added to a flame-dried Schlenk flask under nitrogen. Anhydrous THF (40 mL) and diisopropylamine (8 mL) were then added through the septum with a syringe. The reaction mixture was allowed to reflux overnight. After cooling to room temperature, the mixture was poured into water and was extracted with CH_2Cl_2 (3 × 100 mL). The organic layers were combined, washed with water (5 × 200 mL), and dried over anhydrous sodium sulfate. The solvent was removed and the solid residue was chromatographed on a silica gel column, eluting with CH_2Cl_2. The product was recrystallized from benzene or methylene chloride/hexane.

2,7-Bis[(4-nitrophenyl)ethynyl]-9,10-anthraquinone (2,7-diNO_2) was synthesized from 2,7-dibromo-9,10-anthraquinone (0.29 g, 0.8 mmol) and *p*-ethynylnitrobenzene (0.29 g, 2.0 mmol): yield 0.22 g (56%); mp 292 °C (dec); ^{1}H NMR (400 MHz, $CDCl_3$) δ 8.51 (d, J = 1.47 Hz, 2H), 8.36 (d, J = 8.06 Hz, 2H), 8.28 (d, J = 8.61 Hz, 4H), 7.97 (dd, J = 1.47 Hz, J = 8.06 Hz, 2H), 7.75 (d, J = 8.61 Hz, 4H); IR (KBr) 3107, 3066, 2921, 2846, 2207, 1685, 1595, 1520, 1341, 1286, 1115, 936, 860, 750 cm^{-1}. Anal. Calcd for $C_{30}H_{14}N_2O_6$: C, 72.29; H, 2.83; N, 5.62. Found: C, 72.44; H, 2.89; N, 5.62.

2,7-Bis[(4-methylphenyl)ethynyl]-9,10-anthraquinone (2,7-diCH_3) was synthesized from 2,7-dibromo-9,10-anthraquinone (0.29 g, 0.8 mmol) and *p*-methylphenylacetylene (0.23 g, 2.0 mmol): yield 0.19 g (54%); mp 283−285 °C; ^{1}H NMR (400 MHz, $CDCl_3$) δ 8.44 (d, J = 2.00 Hz, 2H), 8.30 (d, J = 8.00 Hz, 2H), 7.90 (dd, J = 2.00 Hz, J = 8.00 Hz, 2H), 7.48 (d, J = 8.00 Hz, 4H), 7.20 (d, J = 8.00 Hz, 4H), 2.40 (s, 6H); IR (KBr) 3053, 3033, 2925, 2220, 1669, 1589, 1320, 1287, 1253, 937, 870, 743 cm^{-1}. Anal. Calcd for $C_{32}H_{20}O_2$: C, 88.05; H, 4.62. Found: C, 88.15; H, 4.57.

2,7-Bis[(4-methoxyphenyl)ethynyl]-9,10-anthraquinone (2,7-diOCH_3) was synthesized from 2,7-dibromo-9,10-anthraquinone (0.29 g, 0.8 mmol) and *p*-methoxyphenylacetylene (0.26 g, 2.0 mmol): yield 0.24 g (64%); mp 238−239 °C; ^{1}H NMR (400 MHz, $CDCl_3$) δ 8.42 (d, J = 1.65 Hz, 2H), 8.29 (d, J = 8.06 Hz, 2H), 7.88 (dd, J = 1.83 Hz, J = 8.06 Hz, 2H), 7.53 (d, J = 8.79 Hz, 4H), 6.93 (d, J = 8.98 Hz, 4H), 3.859 (s, 6H); IR (KBr) 3066, 2972, 2838, 2207, 1683, 1596, 1508, 1334, 1300, 1240, 1186, 1045, 931, 877, 837, 743 cm^{-1}. Anal. Calcd for $C_{32}H_{20}O_4$: C, 82.04; H, 4.30. Found: C, 82.06; H, 4.25.

(32) Kosynkin, D. V.; Tour, J. M. *Organic Lett.* **2001**, *3*, 993−995.

2,7-Bis[[4-(cyanomethyl)phenyl]ethynyl]-9,10-anthraquinone (2,7-diCH_2CN) was synthesized from 2,7-dibromo-9,10-anthraquinone (0.29 g, 0.8 mmol) and the mixture of *p*-(cyanomethyl)phenylacetylene and *p*-bromobenzonitrile (0.58 g, containing approximately 2.5 mmol of *p*-(cyanomethyl)-phenylacetylene and 0.5 mmol of *p*-bromobenzonitrile): yield 0.26 g (67%); mp 288−290 °C; ^{1}H NMR (400 MHz, $CDCl_3$) δ 8.47 (d, J = 1.46 Hz, 2H), 8.325(d, J = 8.06 Hz, 2H), 7.93 (dd, J = 1.46 Hz, J = 8.06 Hz, 2H), 7.61 (d, J = 8.06 Hz, 4H), 7.39 (d, J = 8.24 Hz, 4H), 3.82 (s, 4H). Anal. Calcd for $C_{34}H_{18}N_2O_2$: C, 83.94; H, 3.73; N, 5.76. Found: C, 83.11; H, 3.87; N, 5.87.

2,7-Bis(phenylethynyl)-9,10-anthraquinone (2,7-diH) was synthesized from 2,7-dibromo-9,10-anthraquinone (0.29 g, 0.8 mmol) and phenylacetylene (0.204 g, 2.0 mmol): yield 0.27 g (82%); mp 258−260 °C; ^{1}H NMR (400 MHz, $CDCl_3$) δ 8.46 (d, J = 1.28 Hz, 2H), 8.31 (d, J = 8.06 Hz, 2H), 7.92 (dd, J = 1.65 Hz, J = 8.05 Hz, 2H), 7.61−7.58 (m, 4H), 7.42−7.40 (m, 6H); IR (KBr) 3066, 3024, 2214, 1678, 1589, 1321, 1279, 1266, 929, 860, 764, 737, 695 cm^{-1}. Anal. Calcd for $C_{30}H_{16}O_2$: C, 88.22; H, 3.95. Found: C, 88.10; H, 3.99.

2,7-Bis[[4-(methylthio)phenyl]ethynyl]-9,10-anthraquinone (2,7-diSCH_3) was synthesized from 2,7-dibromo-9,-10-anthraquinone (0.29 g, 0.8 mmol) and *p*-(thiomethyl)-phenylacetylene (0.30 g, 2.0 mmol): yield 0.16 g (40%); mp 248−249 °C; ^{1}H NMR (400 MHz, $CDCl_3$) δ 8.43 (d, J = 1.28 Hz, 2H), 8.30 (d, J = 8.06 Hz, 2H), 7.89 (dd, J = 1.65 Hz, J = 8.06 Hz, 2H), 7.49 (d, J = 8.42 Hz, 4H), 7.25 (d, J = 8.61 Hz, 4H), 2.52 (s, 6H); IR (KBr) 3079, 3038, 2921, 2214, 1678, 1589, 1506, 1341, 1286, 1094, 929, 867, 819, 737, 668 cm^{-1}. Anal. Calcd for $C_{32}H_{20}S_2O_2$: C, 76.77; H, 4.03. Found: C, 75.62; H, 3.97.

2,7-Bis[[4-(dimethylamino)phenyl]ethynyl]-9,10-anthraquinone (2,7-di$N(CH_3)_2$) was synthesized from 2,7-dibromo-9,10-anthraquinone (0.29 g, 0.8 mmol) and *p*-(dimethylamino)phenylacetylene (0.29 g, 2.0 mmol): yield 0.10 g (25%); mp >330 °C; ^{1}H NMR (400 MHz, $CDCl_3$) δ 8.39 (d, J = 1.65 Hz, 2H), 8.26 (d, J = 8.05 Hz, 2H), 7.84 (dd, J = 1.65 Hz, J = 8.05 Hz, 2H), 7.46 (d, J = 8.97 Hz, 4H), 6.69 (d, J = 8.98 Hz, 4H), 3.03 (s, 12H); IR (KBr) 3100, 2919, 2804, 2203, 1683, 1589, 1522, 1381, 1320, 1273, 1199, 931, 863, 816, 749 cm^{-1}. Anal. Calcd for $C_{34}H_{26}N_2O_2$: C, 82.57; H, 5.30; N, 5.66. Found: C, 80.98; H, 5.09; N, 5.46.

2,7-Bis[(4-acetylphenyl)ethynyl]-9,10-anthraquinone (2,7-di$COCH_3$) was synthesized from 2,7-dibromo-9,10-anthraquinone (0.29 g, 0.8 mmol) and *p*-acetylphenylacetylene (0.29 g, 2.0 mmol): yield 0.14 g (35%); mp 278−279 °C; ^{1}H NMR (400 MHz, $CDCl_3$) δ 8.48 (d, J = 1.29 Hz, 2H), 8.33 (d, J = 8.06 Hz, 2H), 7.99 (d, J = 8.61 Hz, 4H), 7.94 (dd, J = 1.65 Hz, J = 8.06 Hz, 2H), 7.67 (d, J = 8.60 Hz, 4H), 2.64 (s, 6H); IR (KBr) 3079, 3031, 2214, 1692, 1602, 1348, 1273, 956, 936, 833, 744, 668 cm^{-1}. Anal. Calcd for $C_{34}H_{20}O_4$: C, 82.91; H, 4.09. Found: C, 80.97; H, 4.02.

2,7-Bis[[4-(dimethylthio)phenyl]ethynyl]-9,10-anthraquinone borontetrafluoride (2,7-di$S(CH_3)_2^+$) was prepared as follows. 2,7-diSCH_3 (50 mg) was suspended with 10 equiv of $(CH_3)_3OBF_4$ in nitromethane (20 mL). After stirring overnight at room temperature the mixture turned clear. The excess of $(CH_3)_3OBF_4$ was destroyed with methanol (1 mL) and the product was precipitated with CH_2Cl_2. The product was filtered and dried under vacuum: yield 52 mg (98%); mp 290−292 °C (dec); ^{1}H NMR (400 MHz, CD_3CN) δ 8.45 (d, J = 1.64 Hz, 2H), 8.33 (d, J = 8.06 Hz, 2H), 8.05 (dd, J = 1.65 Hz, J = 8.05 Hz, 2H), 7.93 (m, 8H), 3.15 (s, 12H); IR (KBr) 3070, 3033, 2929, 2213, 1683, 1589, 1501, 1327, 1287, 1260, 1058, 931, 877, 823, 743, 662 cm^{-1}. Anal. Calcd for $C_{34}H_{26}S_2O_2B_2F_8$: C, 57.98; H, 3.72. Found: C, 57.85; H, 3.58.

2,6-Dibromo-9,10-anthraquinone. Anhydrous copper(II) bromide (13.6 g, 61 mmol), *tert*-butyl nitrite (8.6 mL, 72 mmol), and anhydrous acetonitrile (300 mL) were mixed together in a three-necked round-bottom flask and the mixture was heated to 80 °C. 2,6-Diamino-9,10-anthraquinone (5.8 g, 24 mmol) was added slowly over a period of 10 min. After nitrogen evolution had subsided, the reaction mixture was cooled to room temperature and was poured into an aqueous solution of HCl (200 mL, 20% w/v). The precipitate was filtered and washed with water (5 × 200 mL), dried under vacuum, and chromatographed on a silica gel column eluting with CH_2Cl_2. The product was recrystallized from benzene: yield 3.4 g (38%); mp 265−268 °C (lit.[10] mp 282−283 °C, lit.[33] mp 289−290 °C); ^{1}H NMR (400 MHz, $CDCl_3$) δ 8.44 (d, J = 2.01 Hz, 2H), 8.17 (d, J = 8.24 Hz, 2H), 7.94 (dd, J = 2.01 Hz, J = 8.24 Hz, 2H); ^{13}C NMR (100 MHz, $CDCl_3$) δ 181.308, 137.410, 134.336, 131.763, 130.382, 130.207, 129.160; IR (KBr) 3093, 3031, 1685, 1582, 1314, 1286, 1169, 1121, 1073, 970, 922, 874, 826, 737, 709, 675 cm^{-1}.

General Procedure for the Synthesis of 2,6-Bis(4-arylethynyl)-9,10-anthraquinones. These compounds were synthesized by procedures analogous to those used for the synthesis of the 2,7-bis(4-arylethynyl)-9,10-anthraquinones.

2,6-Bis[(4-methoxyphenyl)ethynyl]-9,10-anthraquinone (2,6-diOCH_3) was synthesized from 2,6-dibromo-9,10-anthraquinone (0.29 g, 0.8 mmol) and *p*-methoxyphenylacetylene (0.29 g, 2.0 mmol): yield 0.25 g (52%); mp 275−277 °C; ^{1}H NMR (400 MHz, $CDCl_3$) δ 8.41 (s, 2H), 8.30 (d, J = 8.05 Hz, 2H), 7.89 (d, J = 8.06 Hz, 2H), 7.53 (d, J = 8.06 Hz, 4H), 6.93 (d, J = 8.24 Hz, 4H), 3.86 (s, 6H); IR (KBr) 3079, 3011, 2935, 2846, 2214, 1685, 1602, 1520, 1341, 1300, 1259, 116, 1039, 833 cm^{-1}. Anal. Calcd for $C_{32}H_{20}O_4$: C, 82.04; H, 4.30. Found: C, 81.68; H, 4.17.

2,6-Bis(phenylethynyl)-9,10-anthraquinone (2,6-diH) was synthesized from 2,6-dibromo-9,10-anthraquinone (0.29 g, 0.8 mmol) and phenylacetylene (0.21 g, 2.0 mmol): yield 0.25 g (61%); mp 289−290 °C (dec); ^{1}H NMR (400 MHz, $CDCl_3$) δ 8.45 (d, J = 1.65 Hz, 2H), 8.32 (d, J = 8.06 Hz, 2H), 7.92 (dd, J = 1.65 Hz, J = 8.06 Hz, 2H), 7.59 (m, 4H), 7.40 (m, 6H); IR (KBr) 3079, 2214, 1678, 1595, 1334, 1273, 991, 915, 888, 853, 757, 689 cm^{-1}. Anal. Calcd for $C_{30}H_{16}O_2$: C, 88.22; H, 3.95. Found: C, 88.02; H, 3.91.

2,6-Bis[[4-(methylthio)phenyl]ethynyl]-9,10-anthraquinone (2,6-diSCH_3) was synthesized from 2,6-dibromo-9,-10-anthraquinone (0.29 g, 0.8 mmol) and *p*-(methylthio)-phenylacetylene (0.30 g, 2.0 mmol): yield 0.20 g (40%); mp 232−234 °C; ^{1}H NMR (400 MHz, $CDCl_3$) δ 8.42 (d, J = 1.65 Hz, 2H), 8.30 (d, J = 8.06 Hz, 2H), 7.89 (dd, J = 1.65 Hz, J = 8.06 Hz, 2H), 7.50 (d, J = 8.42 Hz, 4H), 7.25 (d, J = 8.42 Hz, 4H), 2.52 (s, 6H); IR (KBr) 3066, 2928, 2221, 1685, 1589, 1492, 1341, 1307, 1279, 1087, 819, 750, 716 cm^{-1}. Anal. Calcd for $C_{32}H_{20}S_2O_2$: C, 76.77; H, 4.03. Found: C, 75.46; H, 3.84.

2-Bromo-9,10-anthraquinone. Anhydrous copper(II) bromide (6.8 g, 30.5 mmol), *tert*-butyl nitrite (4.3 mL, 36 mmol), and anhydrous acetonitrile (200 mL) were mixed together in a three-neck round-bottom flask, and the mixture was heated to 80 °C. 2-Aminoanthraquinone (5.35 g, 36 mmol) was added slowly over a period of 10 min. After nitrogen evolution had subsided, the reaction mixture was cooled to room temperature and was poured into an aqueous solution of HCl (200 mL, 20%, w/v). The precipitate was filtered, washed with water (5 × 200 mL), dried under vacuum, and chromatographed on a silica gel column eluting with CH_2Cl_2. The product was recrystallized from benzene: yield 3.0 g, (43%); mp 206−207 °C (lit.[34] mp 209 °C); ^{1}H NMR (400 MHz, $CDCl_3$) δ 8.44 (d, J = 2.02 Hz, 1H), 8.31 (m, 2H), 8.18 (d, J = 8.24 Hz, 1H), 7.92 (dd, J = 2.02 Hz, J = 8.24 Hz, 1H), 7.83 (m, 2H); ^{13}C NMR (100 MHz, $CDCl_3$) δ 182.344, 181.979, 137.132, 134.522, 134.453, 134.324, 133.277, 133.148, 132.070, 130.211, 129.725, 129.004, 127.372, 127.327; IR (KBr) 3073, 1690, 1582, 1334, 1293, 1172, 1078, 964, 931, 857, 709, 649 cm^{-1}.

General Procedure for the Synthesis of 2-Arylethynyl-9,10-anthraquinones. These compounds were synthesized by procedures analogous to those used for the synthesis of the 2,6- and the 2,7-bis(4-ethynylaryl)-9,10-anthraquinones. They were recrystallized from CH_2Cl_2/hexane.

(33) *Rodd's Chemistry of Carbon Compounds*, 2nd ed.; Coffey, S., Ed.; Elsevier: Amsterdam, 1979; vol. III, part H.

(34) Allen, N. S.; Pullen, G.; Shah, M.; Edge, M.; Holdsworth, D.; Weddel, I.; Swart, R.; Catalina, F. *J. Photochem. Photobiol. A: Chem.* **1995**, *91*, 73−79.

2-[(4-Methylphenyl)ethynyl]-9,10-anthraquinone (2-CH_3) was synthesized from 2-bromo-9,10-anthraquinone (0.29 g, 1 mmol) and *p*-methylphenylacetylene (0.174 g, 1.5 mmol): yield 0.20 g (61%); mp 170−171 °C (lit.[12] mp 172 °C); ^{1}H NMR (400 MHz, $CDCl_3$) δ 8.43 (d, J = 1.65 Hz, 1H), 8.34−8.31 (m, 2H), 8.30 (d, J = 8.06 Hz, 1H), 7.89 (dd, J = 1.65 Hz, J = 8.06 Hz, 1H), 7.83−7.81 (m, 2H), 7.48 (d, J = 8.06 Hz, 2H), 7.20 (d, J = 8.24 Hz, 2H), 2.40 (s, 3H); ^{13}C NMR (100 MHz, $CDCl_3$) δ 182.662, 182.488, 139.508, 136.381, 134.264, 134.135, 133.573, 133.436, 132.131, 131.805, 130.127, 129.892, 129.292, 127.357, 127.304, 127.24, 119.198, 94.714, 87.572, 21.596; IR (KBr) 3080, 2919, 2213, 1676, 1596, 1320, 1280, 931, 857, 830, 716 cm^{-1}. Anal. Calcd for $C_{23}H_{14}O_2$: C, 85.70; H, 4.38. Found: C, 85.65; H, 4.39.

2-(Phenylethynyl)-9,10-anthraquinone (2-H) was synthesized from 2-bromo-9,10-anthraquinone (0.29 g, 1 mmol) and phenylacetylene (0.15 g, 1.5 mmol): yield 0.12 g, (38%); mp 214−215 °C (lit.[11,12] mp 214.5−215.5 °C); ^{1}H NMR (400 MHz, $CDCl_3$) δ 8.45 (d, J = 1.65 Hz, 1H), 8.35−8.33 (m, 2H), 8.31 (J = 8.06 Hz, 1H), 7.91 (dd, J = 1.65 Hz, J = 8.06 Hz, 1H), 7.84−7.82 (m, 2H), 7.61−7.58 (m, 2H), 7.41−7.40 (m, 3H); ^{13}C NMR (100 MHz, $CDCl_3$) δ 182.625, 182.480, 136.465, 134.286, 134.172, 133.558, 133.459, 133.414, 132.298, 131.896, 130.233, 129.641, 129.163, 128.511, 127.380, 127.327, 127.296, 12.280, 94.327, 88.043; IR (KBr) 3073, 2214, 1692, 1589, 1348, 1334, 1286, 977, 936, 867, 778, 716 cm^{-1}. Anal. Calcd for $C_{22}H_{12}O_2$: C, 85.70; H, 3.92. Found: C, 85.85; H, 3.94.

2-[(4-Methoxyphenyl)ethynyl]-9,10-anthraquinone (2-OCH_3) was synthesized from 2-bromo-9,10-anthraquinone (0.29 mg, 1 mmol) and *p*-methoxyphenylacetylene (0.20 g, 1.5 mmol): yield 0.25 g (74%); mp 192−193 °C; ^{1}H NMR (400 MHz, $CDCl_3$) δ 8.42 (d, J = 1.65 Hz, 1H), 8.34−8.32 (m, 2H), 8.29 (d, J = 8.06 Hz, 1H), 7.88 (dd, J = 1.65 Hz, J = 8.06 Hz, 1H), 7.83−7.81 (m, 2H), 7.53 (d, J = 8.88 Hz, 2H), 6.92 (d, J = 8.88 Hz, 2H), 3.86 (s, 3H); ^{13}C NMR (100 MHz, $CDCl_3$) δ 182.700, 182.480, 160.341, 136.229, 134.248, 134.112, 133.588, 133.474, 133.429, 131.979, 130.067, 129.960, 127.349, 127.289, 127.266, 114.318, 114.189, 94.744, 87.125, 55.347; IR (KBr) 2969, 2860, 2214, 1685, 1595, 1520, 1348, 1293, 1252, 1163, 1032, 943, 840, 723 cm^{-1}. Anal. Calcd for $C_{23}H_{14}O_3$: C, 81.64; H, 4.17. Found: C, 81.03; H, 4.07.

2-[(4-Nitrophenyl)ethynyl]-9,10-anthraquinone (2-NO_2) was synthesized from 2-bromo-9,10-anthraquinone (0.29 g, 1 mmol) and *p*-ethynylnitrobenzene (0.22 g, 1.5 mmol): yield 0.13 g (36%); mp 211 °C (dec); ^{1}H NMR (400 MHz, $CDCl_3$) δ 8.46 (d, J = 1,65 Hz, 1H), 8.33−8.31 (m, 3H), 8.25 (d, J = 8.97 Hz, 2H), 7.92 (dd, J = 1.65 Hz, J = 8.06 Hz, 1H), 7.83 (m, 2H), 7.72 (d, J = 8.97 Hz, 2H); ^{13}C NMR (100 MHz, $CDCl_3$) δ 182.397, 182.336, 147.568, 136.601, 134.453, 134.355, 133.550, 133.474, 133.322, 133.019, 132.632, 130.598, 129.065, 128.230, 127.532, 127.387, 123.775, 92.597, 91.640; IR (KBr) 3114, 3079, 2928, 220, 1678, 1595, 1513, 1334, 1286, 1115, 936, 860, 709 cm^{-1}. Anal. Calcd for $C_{22}H_{11}NO_4$: C, 74.78; H, 3.14; N, 3.96. Found: C, 74.81; H, 3.16; N, 4.43.

2,6-Dibromo-9,10-diacetoxyanthracene. 2,6-Dibromoanthraquinone (0.72 g, 2 mmol), activated Zn (0.4 g, 6 mmol), anhydrous sodium acetate (0.2 g, 2.5 mmol), and 30 mL of acetic anhydride were mixed in a round-bottom flask and stirred at room temperature under N_2 until the color changed to green (15 min). The mixture was then heated to reflux until the color changed back to yellow (ca. 1 h). The mixture was cooled, and water (50 mL) was added slowly. The mixture was then boiled again to hydrolyze the acetic anhydride. The precipitate was filtered, washed with water (5 × 50 mL), and dried in a vacuum oven. The product was purified by chromatography on a silica gel column, eluting with methylene chloride: yield 0.62 g (69%); mp 326−327 °C (lit.[10] mp 310 °C); ^{1}H NMR (400 MHz, $CDCl_3$) δ 8.08 (d, J = 1.73 Hz, 2H), 7.79 (d, J = 9.16 Hz, 2H), 7.58 (dd, J = 1.73 Hz, J = 9.26 Hz, 2H), 2.65 (s, 6H); ^{13}C NMR (100 MHz, $CDCl_3$) δ 169.130, 139.766, 130.651, 125.080, 123.904, 123.646, 123.190, 121.589, 20.746; IR (KBr) 3080, 3019, 2939, 1770, 1616, 1461, 1360, 1199, 1159, 1072, 1038, 904, 863, 803, 729 cm^{-1}. Anal. Calcd for $C_{18}H_{12}Br_2O_4$: C, 47.82; H, 2.68. Found: C, 47.80; H, 2.66.

General Procedure for the Synthesis of 2,6-Bis(4-arylethynyl)-9,10-diacetoxyanthracene. 2,6-Dibromo-9,10-diacetoxyanthracene (0.5 mmol), phenylacetylene (1.5 mmol) or 4-methoxy phenylacetylene (1.5 mmol), $Pd(PPh_3)_2Cl_2$ (0.05 mmol), and CuI (0.05 mmol) were mixed in a flame-dried Schlenk flask under nitrogen. Anhydrous THF (40 mL) and diisopropylamine (8 mL) were then added with syringe. The reaction mixture was allowed to reflux overnight. The mixture was cooled, poured into water, and extracted with methylene chloride (100 mL). The organic layer was washed with water (5 × 200 mL) and dried over anhydrous sodium sulfate. The solid residue was chromatographed on a silica gel column, eluting with methylene chloride. The product was recrystallized from methylene chloride/hexane.

2,6-Bis[(4-methoxyphenyl)ethynyl]-9,10-diacetoxyanthracene (r-2,6-diOCH_3) was synthesized from 2,6-dibromo-9,10-diacetoxyanthracene (0.36 g, 0.8 mmol) and *p*-methoxyphenylacetylene (0.26 g, 2.0 mmol): yield 0.37 g (84%); mp 270−273 °C; ^{1}H NMR (400 MHz, $CDCl_3$) δ 8.08 (s, 2H), 7.88 (d, J = 9.15 Hz, 2H), 7.58−7.53 (m, 6H), 6.92 (d, J = 8.61 Hz, 4H), 3.85 (s, 6H), 2.67 (s, 6H); ^{13}C NMR (100 MHz, $CDCl_3$) δ 169.320, 159.947, 140.032, 133.254, 129.163, 124.807, 124.306, 123.448, 121.976, 114.956, 114.106, 91.777, 88.475, 55.332, 20.845; IR (KBr) 3079, 3018, 2928, 2207, 1760, 1609, 1520, 1362, 1245, 1183, 1128, 1053, 1025, 833, 812 cm^{-1}. Anal. Calcd for $C_{36}H_{26}O_6$: C, 77.97; H, 4.73. Found: C, 77.47; H, 4.64.

2,6-Bis(phenylethynyl)-9,10-diacetoxyanthracene (r-2,6-diH) was synthesized from 2,6-dibromo-9,10-diacetoxyanthracene (0.36 g, 0.8 mmol) and phenylacetylene (0.20 g, 2.0 mmol): yield 0.33 mg (83%); mp 309 °C (dec); ^{1}H NMR (400 MHz, $CDCl_3$) δ 8.11 (s, 2H), 7.90 (d, J = 8.97 Hz, 2H), 7.62−7.58 (m, 6H), 7.40−7.38 (m, 6H), 2.68 (s, 6H); ^{13}C NMR (100 MHz, $CDCl_3$) δ 169.320, 140.161, 131.767, 129.141, 128.685, 128.450, 125.255, 124.367, 123.570, 122.872, 122.113, 121.741, 91.678, 89.606, 20.845; IR (KBr) 3073, 3018, 2928, 2207, 1753, 1623, 1492, 1362, 1190, 1163, 1046, 826, 771, 680 cm^{-1}. Anal. Calcd for $C_{34}H_{22}O_4$: C, 82.58; H, 4.48. Found: C, 82.11; H, 4.31.

2,7-Dibromo-9,10-diacetoxyanthracene was synthesized by the same procedure used for the synthesis of the 2,6-analogue, using 2,7-dibromoanthraquinone (0.37 g, 1 mmol): yield 0.27 g, (60%); mp 324−325 °C; ^{1}H NMR (400 MHz, $CDCl_3$) δ 8.08 (d, J = 1.46 Hz, 2H), 7.80 (d, J = 9.34 Hz, 2H), 7.57 (dd, J = 1.83 Hz, J = 9.34 Hz, 2H), 2.67 (s, 3H), 2.63 (s, 3H); ^{13}C NMR (100 MHz, $CDCl_3$) δ 169.153, 169.100, 141.102, 138.423, 130.370, 125.596, 123.813, 123.729, 122.659, 121.976, 20.971, 20.678; IR (KBr) 3087, 2932, 1763, 1622, 1569, 1441, 1354, 1199, 1166, 1078, 1038, 964, 810, 776, 729 cm^{-1}. Anal. Calcd for $C_{18}H_{12}Br_2O_4$: C, 47.82; H, 2.68. Found: C, 47.31; H, 2.49.

2,7-Bis[(4-methoxyphenyl)ethynyl]-9,10-diacetoxyanthracene (r-2,7-diOCH_3) was synthesized in analogy to r-2,6-diOCH_3, using 2,7-dibromo-9,10-diacetoxyanthracene (0.36 g, 0.8 mmol) and *p*-methoxyphenylacetylene (0.26 g, 2.0 mmol): yield 0.40 g (89%); mp 266−267 °C; ^{1}H NMR (400 MHz, $CDCl_3$) δ 8.07 (s, 2H), 7.89 (d, J = 8.98 Hz, 2H), 7.59−7.54 (m, 6H), 6.92 (d, J = 8.61 Hz, 4H), 3.85 (s, 6H), 2.70 (s, 3H), 2.64 (s, 3H); ^{13}C NMR (100 MHz, $CDCl_3$) δ 169.388, 169.259, 159.947, 140.381, 139.690, 133.262, 129.133, 124.830, 124.367, 123.395, 122.029, 121.968, 114.956, 114.106, 91.678, 88.422, 55.332, 20.943, 20.731; IR (KBr) 3086, 2956, 2839, 2214, 1767, 1609, 1513, 1376, 1252, 1204, 1053, 881, 833, 771 cm^{-1}. Anal. Calcd for $C_{36}H_{26}O_6$: C, 77.97; H, 4.73. Found: C, 78.03; H, 4.62.

Acknowledgment. We thank the NASA Glenn Research Center Director's Discretionary Fund (DDF) for financial support. We also wish to thank Prof. W. J. Youngs of the University of Akron for his assistance with the X-ray analysis.

Supporting Information Available: Appendix I: Crystallographic data for 2,7-diH; Appendix II: Equilibrium geometries for the first singlet excited states of 2-NO_2, 2-H and 2-OCH_3 (PDF). This material is available free of charge via the Internet at http://pubs.acs.org.

CM049590G